Electronic Supplementary Material (ESI) for Dalton Transactions.

Supporting Information

A Modular Approach to Carbene-Stabilized Diphosphorus Species

Adinarayana Doddi, Dirk Bockfeld, Marc-Kevin Zaretzke, Christian Kleeberg, Thomas Bannenberg
and Matthias Tamm

A) General procedures and analytical methods

B) NMR and other spectra

C) X-ray crystallographic data

D) Computational details

E) References

A) General Procedures and Analytical Methods

All manipulations were performed under a strictly dry argon atmosphere using standard Schlenk line techniques and dry argon- filled glove boxes. Solvents used were dried using the MBraun solvent purification system. ^{1}H, ^{13}C, ^{11}B and ^{31}P-NMR spectra were measured on Bruker AV II 300 (300 MHz), AV III 400 (400 MHz) AV III HD 500 (500 MHz) and Bruker AV II 600 (600 MHz) spectrometers. The chemical shifts are given in parts per million (δ; ppm) relative to residual solvent peaks (δ; 7.15 (C_6D_6), 5.34 (CD_2Cl_2) ppm). Coupling constants (*J*) are reported in Hertz (Hz), and splitting patterns are indicated as s (*singlet*), d (*doublet*), t (*triplet*), m (*multiplet*), sept (*septet*) and br (*broad*). All spectra were measured at room temperature unless otherwise stated. Elemental analyses were carried out on a Elementar Vario Micro Cube System. (IPr)PSiMe$_3$ (**1**)[1] and the carbene-PCl$_3$ adducts (IMes)PCl$_3$[2] and (IPr)PCl$_3$[2] were prepared according to the literature reported procedures. Cyclic voltammetry was performed with a Princeton Applied Research VersaSTAT 3 potentiostat under inert conditions at room temperature in THF with *n*Bu$_4$PF$_6$ as electrolyte. A self-made three electrode set-up was used, consisting of two platinum wires as working and counter electrodes and a silver wire as quasi-reference electrode. Ferrocene was added as internal standard. The X-band EPR spectra were recorded on a Bruker EMX spectrometer with an OXFORD ESR900 continuous flow cryostat. The samples were transferred into a 4 mm diameter quartz EPR tube (Wilmad 707-SQ-250M) and the spectra were simulated with EasySpin 5.1.12.[3] EI mass spectra were recorded on a Thermofinnigan MAT95XL double focusing sectorfield mass spectrometer, ESI mass spectra on a ThermoQuest Finnigan LCQ Deca spectrometer. High resolution electrospray (HR-MS ESI) measurements were performed on ThermoFisher Scientific LTQ-Orbitrap Velos by direct infusion mode using a custom made microspray-device mounted on a Proxeon nanospray ion source. The cation of tetradecylammonium bromide was used as internal mass reference.

X-ray Structure Determinations

Suitable single crystals were mounted on glass fibers (**4**, **[5][PF$_6$]** polymorph A, **[5][BF$_4$]**) or human hair (**3**, **[5][PF$_6$]** Polymorph B, **[6][GaCl$_4$]**, **[6][BAr^F]**) in perfluorinated inert oil. Intensity measurements were performed at 100 K (**[5][PF$_6$]** polymorph B at 200 K) using an Oxford Diffraction Xcalibur Nova A diffractometer with mirror-focused Cu*Kα* radiation. Absorption corrections were based on multi-scans. Additional Gaussian absorption correction by face indexation was applied on **4**, **[5][PF$_6$]** Polymorph A, **[5][PF$_6$]** Polymorph B and **[5][BF$_4$]**). For data collections and reductions the software CrysAlisPro was used.[4] The structure of **4** was solved by direct methods with SHELXS-14.[5a] All other crystal structures were solved by intrinsic phasing with SHELXT-2014.[5b] SHELXL-2014 was applied for the anisotropic refinement on F^2 data.[5a] Further details can be found in the X-ray crystallographic data section below.

Synthesis of [(IPr)PP(Cl)(IMes)]Cl (3)

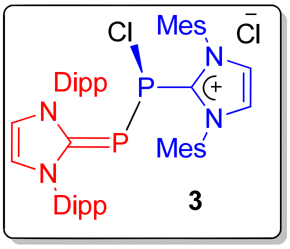

3

To a solution of (IMes)PCl$_3$ (**2**, 0.180 g, 0.406 mmol) in toluene (10 mL) a toluene (10 mL) solution of [(IPr)PSi(CH$_3$)$_3$] (**1**, 0.200 g, 0.406 mmol) was added while stirring at ambient temperature. The resulting dark green solution was then heated to 80 °C for 90 min during which formation of a brown precipitate was observed. All volatiles were removed under reduced pressure, washed the residue with *n*-hexane (6 x 5 mL), then dried under vacuum to get **3**. Yield: 0.257 g (77 %). ^{1}H NMR (400 MHz, CD$_2$Cl$_2$): δ = 7.35 (t, 2H, J_{HH} = 7.3 Hz, Ar-*H*), 7.38 (d, 1H, J_{HH} = 7.3 Hz, Ar-*H*), 7.24–7.21 (m, 4H, Ar-*H*), 7.17-7.10 (m, 4H, Ar-*H*, IMes), 6.91 (br, 2H, N$_2$C$_2$-*H*, IPr), 6.76 (br, 2H, N$_2$C$_2$-*H*, IMes), 2.43 (sept, J_{HH} = 6.8 Hz, C*H*(CH)$_3$), 2.38-235 (brm, 5H (2H (C*H*(CH)$_3$ + 3H *m*-CH$_3$), 2.31 (brs, 6H, *m*-CH$_3$), 2.20 (s, 3H, *m*-C*H*$_3$), 1.91 (brs, 3H, *p*-C*H*$_3$), 1.80 (brs, 3H, *p*-C*H*$_3$), 1.27 (d, 3H, J_{HH} = 6.8 Hz, CH(C*H*)$_3$), 1.26 (d, 3H, J_{HH} = 6.8 Hz, CH(C*H*)$_3$), 1.09 (d, 12H, J_{HH} = 6.7 Hz, CH(C*H*)$_3$), 0.95 (broad doublet, 6H, CH(C*H*)$_3$) ppm. ^{31}P NMR (121.5 MHz, CD$_2$Cl$_2$): δ = 137.95 (d, J_{PP} = 381 Hz, (IMes)*P*) and –22.07 (d, J_{PP} = 381 Hz, (IPr)*P*) ppm. HR-MS (ESI, in CH$_3$CN, positive ion mode, m/z) for the cationic moiety [(IPr)P$_2$(Cl)(IMes)]$^+$: 789.3971 (calcd 789.3976). Anal. Calcd (%) for C$_{48}$H$_{60}$Cl$_2$N$_4$P$_2$·C$_7$H$_8$; C 72.01, H 7.47, and N 6.11; Found: C 72.11, H 7.56 and N 5.99. **Minor isomer 3'**: ^{31}P NMR (121.5 MHz, CD$_2$Cl$_2$): δ = 128.42 (d, J_{PP} = 373 Hz, (IMes)*P*) and –28.31(d, J_{PP} = 373 Hz, (IPr)*P*) ppm. *Note*: Compound **3** slowly decomposes in CD$_2$Cl$_2$ and ^{1}H NMR spectra always showed the formation of the corresponding imidazolium salts [(IPr)HCl and (IMes)HCl]. This material was used without further purification in the preparation of other compounds.

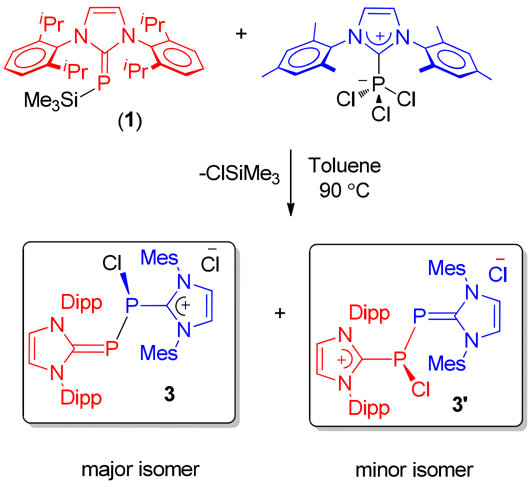

Scheme S1: Synthesis dicarbene phosphorus dichloride **3**.

Synthesis of [(IPr)PPCl(IPr)]Cl

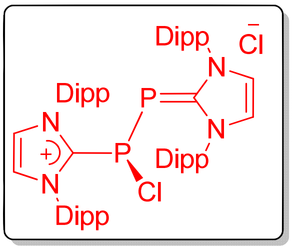

To a clear yellow solution of (IPr)PSiMe$_3$ (**1**, 0.120 g, 0243 mmol) in benzene (15 mL) (IPr)PCl$_3$ (0.128 g, 0243 mmol) was added while stirring at room temperature. The dark green solution was stirred for 2.30 h at the same temperature. The precipitate was then filtered and washed with small amount of THF (1 mL x 2) followed by *n*-hexane and dried under vacuum to get [(IPr)PPCl(IPr)]Cl as yellow-brown solid. Yield: 0.112 g (50%). ^{1}H NMR (CD$_2$Cl$_2$, 500 MHz): 7.63 (s, 2H, $H_2\mathrm{N_2C_2}$, (IPr)PCl), 7.50 (t, 2H, J_{HH} = 7.4 Hz, *p*-Ar(*H*)), 7.46 (t, 2H, J_{HH} = 7.4 Hz, *p*-Ar(*H*)), 7.31-7.29 (m, 2H, *m*-Ar(*H*)), 7.24-7.23 (m, 2H, *m*-Ar(*H*)), 7.15-7.13 (m, 4H, *m*-Ar(*H*)), 7.02 (s, 2H, $H_2\mathrm{N_2C_2}$), 2.46-2.41 (m, 4H, $\mathrm{C}H(\mathrm{CH_3})_2$), 2.32 (sept, 2H, J_{HH} = 6.8 Hz, $\mathrm{C}H(\mathrm{CH_3})_2$), 2.19 (sept, 2H, J_{HH} = 6.8 Hz, $\mathrm{C}H(\mathrm{CH_3})_2$), 1.21 (d, 6H, J_{HH} = 6.8 Hz, $\mathrm{CH}(CH_3)_2$), 1.18 (d, 6H, J_{HH} = 6.8 Hz, $\mathrm{CH}(CH_3)_2$), 1.05 (d, 6H, J_{HH} = 6.9 HZ, $\mathrm{CH}(CH_3)_2$), 1.07 (d, 6H, J_{HH} = 6.9 HZ, $\mathrm{CH}(CH_3)_2$), 1.04 (d, 6H, J_{HH} = 6.9 HZ, $\mathrm{CH}(CH_3)_2$), 1.01 (d, 6H, J_{HH} = 6.8 Hz, $\mathrm{CH}(CH_3)_2$), 0.85 (d, 6H, J_{HH} = 6.9 HZ, $\mathrm{CH}(CH_3)_2$), 0.75 (d, 6H, J_{HH} = 6.8 Hz, $\mathrm{CH}(CH_3)_2$) ppm. ^{13}C NMR (125.8 MHz, CD$_2$Cl$_2$): δ = 166.7 (d, J_{PC} = 34 Hz, ClP–C_{NHC}), 165.7 (d, J_{PC} = 34 Hz, P–C_{NHC}), 147.61 (N*C*(Dipp), 146.81 (N*C*(Dipp), 146.05 (*o*-*C*(Dipp), 145.94 (*o*-*C*(Dipp), 145.82 (*o*-*C*(Dipp), 132.90 (*p*-*C*(Dipp), 132.18 (*p*-*C*(Dipp), 127.96 ($C_2\mathrm{H_2N_2}$), 125.92 (*m*-*C*(Dipp), 125.64 (*m*-*C*(Dipp), 125.54 (*m*-*C*(Dipp), 125.46 (d, J_{PC} = 3.7 Hz, $C_2\mathrm{H_2N_2}$),124.82 (*m*-*C*(Dipp), 29.91 ($C\mathrm{H(CH)_3}$), 29.84 ($C\mathrm{H(CH)_3}$), 29.82 ($C\mathrm{H(CH)_3}$), 29.63 ($C\mathrm{H(CH)_3}$), 26.52 ($\mathrm{CH}(C\mathrm{H})_3$), 26.07 ($\mathrm{CH}(C\mathrm{H})_3$), 26.12 ($\mathrm{CH}(C\mathrm{H})_3$), 25.24 ($\mathrm{CH}(C\mathrm{H})_3$), 23.72 ($\mathrm{CH}(C\mathrm{H})_3$), 23.54 ($\mathrm{CH}(C\mathrm{H})_3$), 22.23 ($\mathrm{CH}(C\mathrm{H})_3$) and 23.19 ($\mathrm{CH}(C\mathrm{H})_3$) ppm. ^{31}P NMR (CD$_2Cl_2$, 162 MHz): δ = 130.4 (d, J_{PP} = 381 Hz, (IPr)*P*–Cl), –23.0 (d, J_{PP} = 381 Hz, (IPr)*P*) ppm. HRMS (ESI, in CH$_3$CN, positive ion mode) for the cationic moiety $\mathrm{C_{54}H_{72}N_4N_2P_2Cl}$: 873.4912 (873.4915). Anal. Calcd (%) for $\mathrm{C_{54}H_{72}Cl_2N_4P_2}$ (910.028 g/mol): C 71.27, 7.97 and N 6.16; found: C 70.89, H 7.63 and N 6.24.

Synthesis of [(IPr)PP(IMes)] (4)

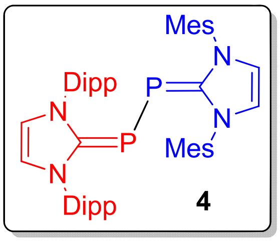

4

To a stirred solution of [(IPr)PPCl(IMes)]Cl (**3**) (0.080 g, 0.096 mmol) in THF (20 mL) potassium graphite (0.030 mg, 0.222 mmol) was added as solid portions. The resulting dark brown-green suspension was stirred at room temperature for 6 h and then filtered to get a dark red solution. All the volatiles were removed under reduced pressure and the red residue was extracted with benzene (*carcinogenic, care should be taken*) (10 mL), and subsequent removal of the solvent afforded **4** as dark red solid. Yield: 0.061 g (84%) based on **3**. ^{1}H NMR (300.1 MHz, $\mathrm{C_6D_6}$): δ = 7.19–7.15 (m, 2H, Ar-*H*, IPr), 6.96 (m, 4H, Ar-*H*, IMes), 6.66 (m, 4H, Ar-*H*, IPr), 5.99 (s, 2H, $\mathrm{N_2C_2}$*H*, IPr), 5.74 (s, 2H, $\mathrm{N_2C_2}$-*H*, IMes), 3.11 (sept, J_{HH} = 6.9 Hz, C*H*(CH)$_3$), 2.21 (s, 6H, IMes-C*H*$_3$), 2.15 (s, 12H, IMes-C*H*$_3$), 1.41 (d, J_{HH} = 6.7 Hz, CH(C*H*)$_3$) and 1.18 (d, J_{HH} = 6.7 Hz, CH(C*H*)$_3$) ppm. ^{13}C NMR (75.5 MHz, $\mathrm{C_6D_6}$): δ =169.8 (brm, P–C_{NHC} (IPr)), 164.8 (brm, P–C_{NHC} (IMes)), 148.4 (N*C*(Dipp), 137.8 (*o*-C(Dipp), 135.6 (N*C*(Mes), 135.1 (*o*-*C*(Mes)), 128.7 (*m*-*C*(Mes)), 128.3 (*p*-*C*(Mes), 129.2 (*p*-*C*(Dipp)), 123.4 ((*m*-*C*(Dipp)), 119.4 (*C*$_2$N$_2$H$_2$, IPr), 117.6 (*C*$_2$N$_2$H$_2$, IMes), 29.2 (*C*H(CH)$_3$), 25.2 (CH(*C*H)$_3$), 23.7 (CH(*C*H)$_3$), 21.8 (*p*-*C*H)$_3$) and 18.9 (*o*-*C*H)$_3$) ppm. ^{31}P NMR (121.47 MHz, $\mathrm{C_6D_6}$): δ = –63.1 (d, J_{PP} = 249 Hz, (IPr)*P*) and –59.40 (d, J_{PP} = 249 Hz, (IMes)*P*) ppm. EI-MS for $\mathrm{C_{48}H_{60}N_4P_2}$ (754.43 g/mol); 754.3 [M]$^+$ (50%). Anal. Calcd (%) for $\mathrm{C_{48}H_{60}N_4P_2}$; C 76.35, H 8.01, and N 7.42; Found: C 76.14, H 8.22 and N 7.19.

Synthesis of [(IPr)P-P(IPr)] (A)

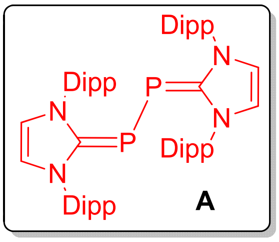

A

To a THF (15 mL) solution of the dicarbene dichloride [(IPr)PPCl(IPr)]Cl (0.050 g, 0.055 mmol) potassium graphite (0.015 g, 0.111 mmol) was added as solid portions at room temperature and. The reaction mixture was vigorously stirred at this temperature for 5.30 h. The solution was then filtered and the solvent removed in vacuo to give **A** as a dark red solid. Yield: 0.041 g (88%). ^{1}H NMR (300.1 MHz, $\mathrm{C_6D_6}$): δ = 7.20-7.16 (m, 4 H, Ar-*H*), 7.01 (d, 8H, Ar-*H*), 5.97 (s, 8H, $\mathrm{N_2C_2}$-*H*), 3.05 (sept, J_{HH} = 6.7 Hz, C*H*(CH)$_3$), 1.36 (d, 24H, J_{HH} = 6.9 Hz, CH(C*H*)$_3$), 1.14 (d, 24H, J_{HH} = 6.9 Hz, CH(C*H*)$_3$) ppm. ^{31}P NMR (121.47 MHz, $\mathrm{C_6D_6}$): δ = –52.29 (s) ppm. ^{13}C NMR (75.5 Hz, $\mathrm{C_6D_6}$): δ = 147.15 [((N*C*(Dipp)], 135.43 [(*o*-*C*(Dipp)], 128.43 (*p*-C(Dipp)), 123.09, 118.81, 28.17

(*C*H(CH$_3$)$_3$), 24.28 (CH(*C*H$_3$)$_3$) and 22.92 (CH(*C*H$_3$)$_3$) ppm. The spectroscopic data are similar to the already reported values.[6]

[(IPr)PP(IMes)][PF$_6$] [5]PF$_6$

A Schlenk tube containing a mixture of NHC-diphosphinidene **4** (0.056 g, 0.074 mmol) and [Fc]PF$_6$ (0.022 g, 0.066 mmol) THF (15 mL) was added as a solvent. The color of the reaction mixture turned to dark green immediately. After the solution was stirred overnight at room temperature, the solvent was removed in vacuo and the residue was washed with toluene (2 mL x 6). The resulting dark green solid was dried under vacuum to give the radical cation **[5]**PF$_6$. Yield: 0.039 g (57%). Anal. Calcd (%) for C$_{48}$H$_{60}$F$_6$N$_4$P$_3$ (899.926 g/mol); C 64.06, H 6.72, and N 6.23; Found: C 63.02, H 6.55 and N 6.14 (*note*; very sensitive to moisture, air and some solvents and better values could not be obtained). ESI-MS (m/z, CH$_3$CN, positive ion mode): 754.50 (754.4293 calcd for C$_{48}$H$_{60}$N$_4$P$_2$). EPR data (CH$_2$Cl$_2$, 298 K, 2.00865 GHz): g_{iso} = 2.00865, A^{31}P =43.33 G, A^{14}N =1.66 G.

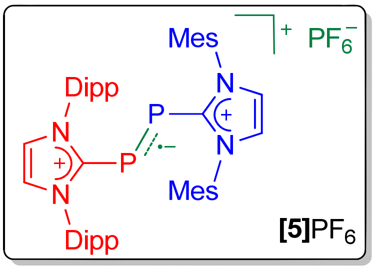

[5]PF$_6$

[(IPr)P=P(IMes)][GaCl$_4$]$_2$ [6][GaCl$_4$]$_2$

To a stirred suspension of [(IPr)PPCl(IMes)]Cl (**3**) (0.045 g, 0.054 mmol) in fluorobenzene (5 mL) GaCl$_3$ (0.019 g, 0.108 mmol) was added as solid portions. The resulting dark orange solution was stirred for 3h at room temperature. An orange micro crystalline precipitate was obtained after filtration and washed with toluene (2 mL x 5). This isolated material was then thoroughly dried under vacuum to give compound **[6]**[GaCl$_4$]$_2$. Yield: 0.042 g (65%). ^{1}H NMR (600.1 MHz, CD$_2$Cl$_2$): δ = 8.19 (s, 2H, N$_2$C$_2$-*H*), 7.98 (s, 2H, N$_2$C$_2$-*H*), 7.69 (t, 2H, J_{HH} = 7.9 Hz, Ar-*H*, IPr), 7.33 (d, 4H, J_{HH} = 7.6 Hz, Ar-*H*, IPr), 7.00 (brm, 4H, Ar-*H*), 2.39 (s, 6H, *p*-C*H$_3$*), 2.10 (sept, 4H, J_{HH} = 7.3 Hz, C*H*(CH)$_3$), 1.83 (s, 12H, *o*-C*H$_3$*), 1.22 (d, 12H, J_{HH} = 6.9 Hz, CH(C*H*)$_3$) and 0.87 (d, 12H, J_{HH} = 6.9 Hz, CH(C*H*)$_3$, IPr) ppm. ^{13}C NMR (150.9 MHz, CD$_2$Cl$_2$): δ = 149.5 (broad doublet, J_{PC} = 72 Hz, P–C$_{NHC}$ (IPr)), 146.7 (broad doublet, J_{PC} = 71 Hz, P–C$_{NHC}$ (IMes)), 145.3 (N*C*(Dipp)), 144.3 (N*C*(Mes)), 134.3 (*p*-*C*(Dipp)), 134.2 (*p*-*C*(Mes)), 131.4 (*m*-*C*(Mes)), 130.6 (N$_2$*C*$_2$H$_2$, IPr), 130.0 (N$_2$*C*$_2$H$_2$, IMes), 129.7 (*o*-*C*(Dipp), 126.5 (*m*-*C*(Dipp)), 29.8 (*C*H(CH)$_3$), 25.2 (CH(*C*H)$_3$), 23.3 (CH(*C*H)$_3$), 21.7 (*p*-*C*H$_3$) and 17.8 (*o*-*C*H$_3$) ppm. ^{31}P NMR (121.5 MHz,

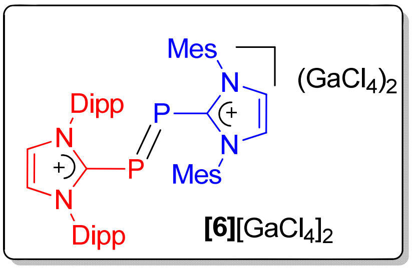

[6][GaCl$_4$]$_2$

CD_2Cl_2): δ = 440.1 (d, J_{PP} = 543 Hz, (IPr)*P*) and 438.5 (d, J_{PP}= 543 Hz, (IMes)*P*) ppm. Anal. Calcd (%) for $C_{48}H_{60}Cl_8Ga_2N_4P_2$; C 48.94, H 5.13, and N 4.76; Found: C 49.47, H 5.55 and N 5.40.

Synthesis of [(IPr)P=P(IMes)][BAr^F]$_2$ [6][BAr^F]$_2$

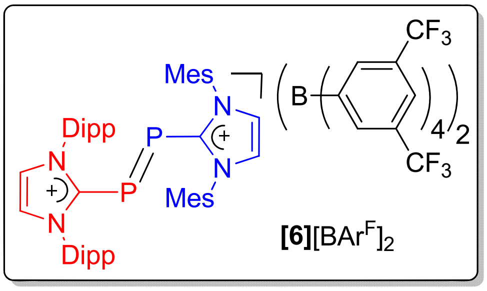

[6][BAr^F]$_2$

In a Schlenk tube dichloromethane (15 mL) was added to a mixture of [(IPr)PPCl(IMes)]Cl (**3**) (0.050 g, 0.060 mmol) and Na[BAr^F] (sodium tetrakis[(3,5-trifluoromethyl)phenyl]borate) (0.107 g, 0.012 mmol) and the reaction solution was stirred for 4 h at room temperature. The resulting solution was filtered and the organic solvent was removed in vacuo. The residue obtained was washed with benzene (2 mL x 5) followed by *n*-hexane and dried under vacuum to obtain **[6]**[BAr^F]$_2$ as an orange solid. Yield: 0.118 g (79%). ^{1}H NMR (300.1 MHz, CD_2Cl_2): δ = 7.91 (s, 2H, N_2C_2-*H*, IPr), 7.75 (s, 2H, N_2C_2-*H*, IMes), 7.74–7.10 (br, 16H, *H*(BAr^F)), 7.63 (t, 2H, J_{HH} = 7.9 Hz, Ar-*H*, IPr), 7.56 (br, 8H, *H*(BAr^F)), 7.30 (d, 4H, J_{HH} = 7.7 Hz, Ar-*H*, IPr), 6.98 (br, 4H, Ar-*H*, IMes), 2.35 (s, 6H, *p*-C*H*$_3$), 2.02 (sept, 4H, J_{HH} = 7.5 Hz, C*H*(CH)$_3$), 1.76 (s, 12H, *o*-C*H*$_3$), 1.15 (d, 12H, J_{HH} = 6.7 Hz, CH(C*H*)$_3$) and 0.85 (d, 12H, J_{HH} = 6.9 Hz, CH(C*H*)$_3$) ppm. ^{13}C NMR (75.5 MHz, CD_2Cl_2): δ = 162.3 (q, $^1J_{BC}$ = 49.3 Hz, *C*-B, B(Ar^F)), 145.1 (N*C*(Dipp)), 145.3 (N*C*(Mes), 135.4 (*o*-*C*(BAr^F), 134.3 (*p*-*C*(Dipp)), 131.8 (*o*-*C*(Mes)), 130.3 ($N_2C_2H_2$, IMes), 129.9 (*m*-*C*(Dipp)), 129.6 (*m*-*C*(IMes)), 129.4 (qq, $^2J_{CF}$ = 30.2 Hz, $^3J_{BC}$ = 3.1 Hz, *m*-*C*-BAr^F), 129.3 (*p*-*C*(IMes), merged with *m*-*C*BAr^F), 128.9 ($N_2C_2H_2$, IPr), 128.7 (q, $^1J_{CF}$ = 272.2 Hz, *C*F$_3$(BAr^F)), 118.1 (sept, $^3J_{FC}$ = 4.0 Hz, *p*-*C*(BAr^F)), 30.1 (*C*H(CH)$_3$), 25.2 (CH(*C*H)$_3$), 23.3 (CH(*C*H)$_3$), 21.7 (*p*-*C*H$_3$) and 17.7 (*o*-*C*H$_3$) ppm. ^{31}P NMR (121.53 MHz, CD_2Cl_2): δ = 442.29 (P–P couplings are not visible at RT) ppm. ^{11}B NMR (96.2 MHz, CD_2Cl_2): δ = –6.43 ppm. Anal. Calcd (%) for $C_{112}H_{84}B_2F_{48}N_4P_2$; C 54.18, H 3.41, and N 2.25; Found: C 53.80, H 3.49 and N 2.29.

……

B) NMR and other spectra of the reported compounds

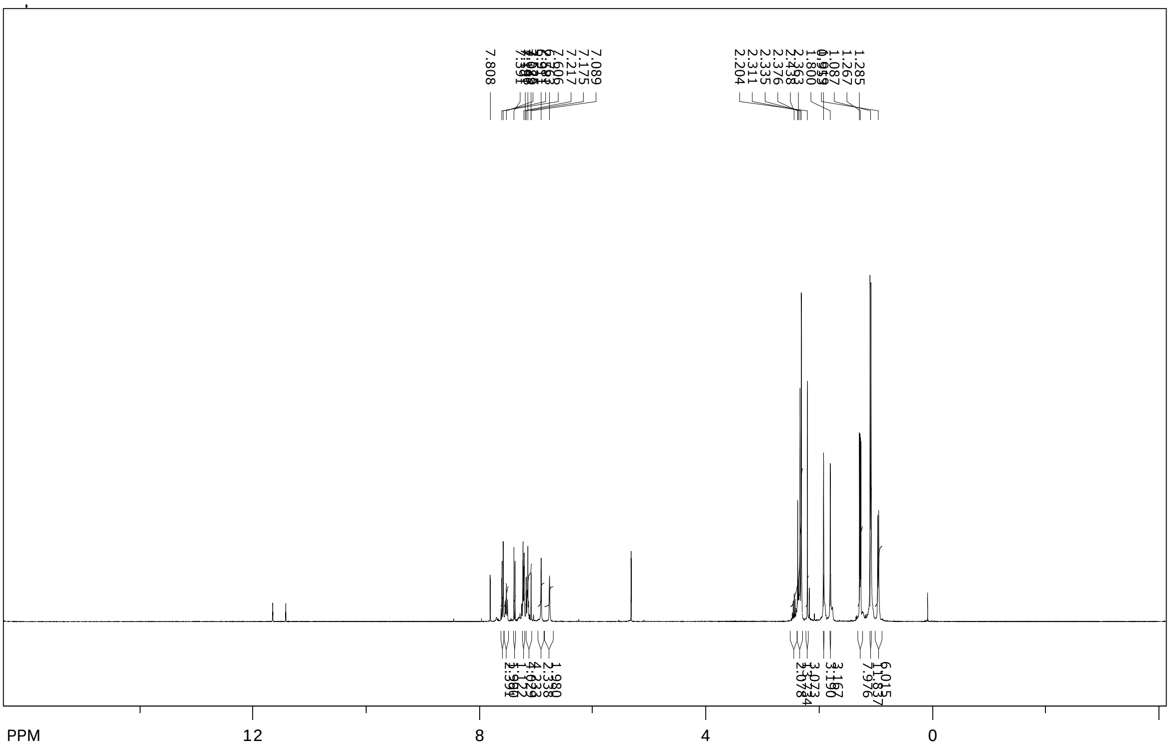

Figure S1: ^{1}H NMR spectrum of [(IPr)PPCl(IMes)]Cl (**3**) in CD_2Cl_2.

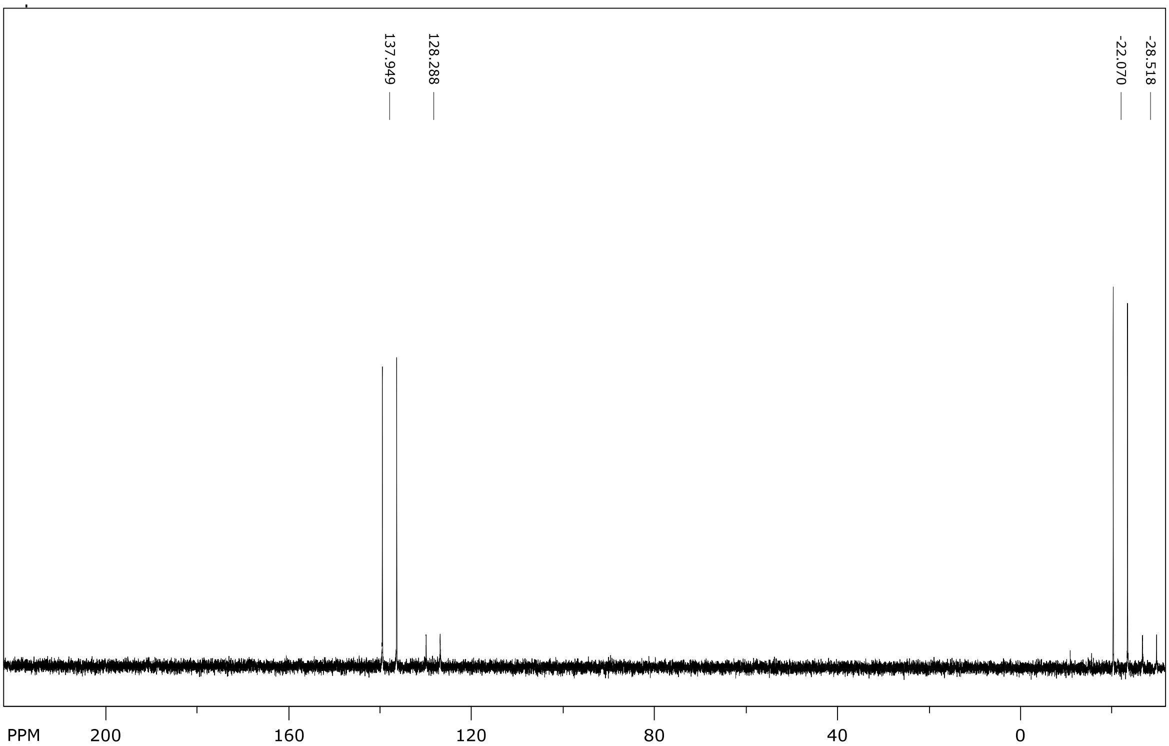

Figure S2: ^{31}P NMR spectrum of [(IPr)PPCl(IMes)]Cl (**3**) in CD_2Cl_2 [δ = 128.28 (d, J_{PP} = 375 Hz, –28.52 (d, J_{PP} = 375 Hz)].

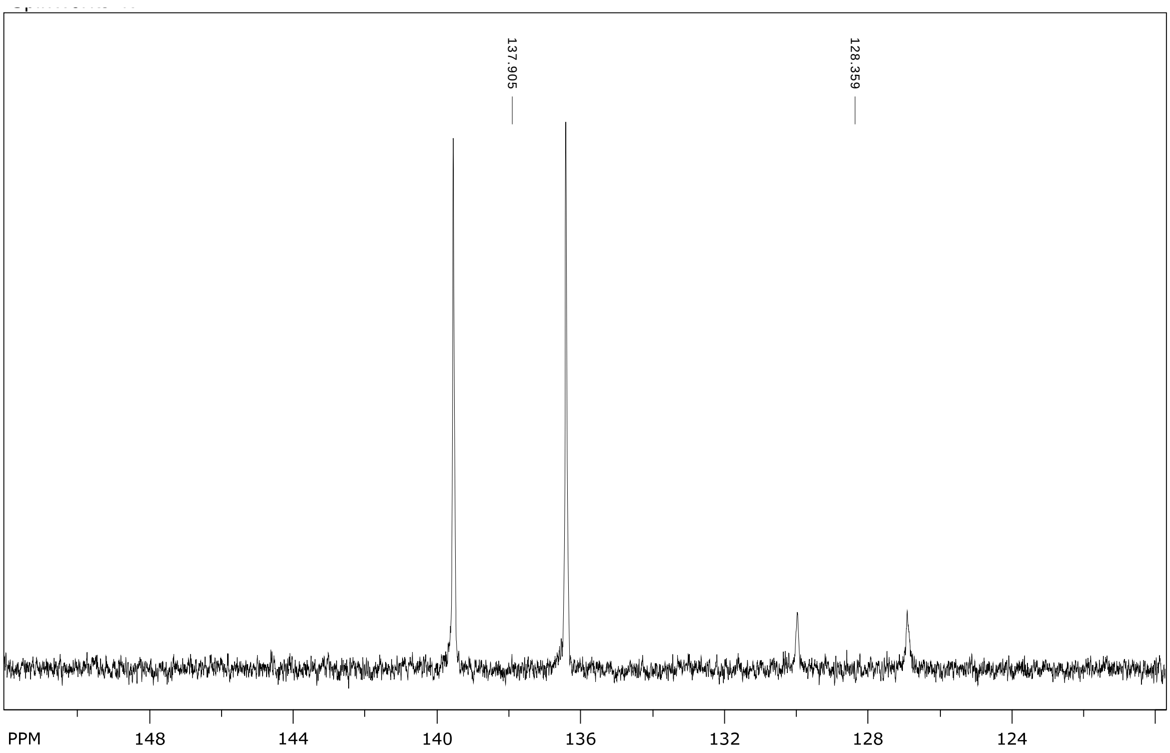

Figure S3: ^{31}P NMR spectrum of [(IPr)PPCl(IMes)]Cl (**3**) (expanded view).

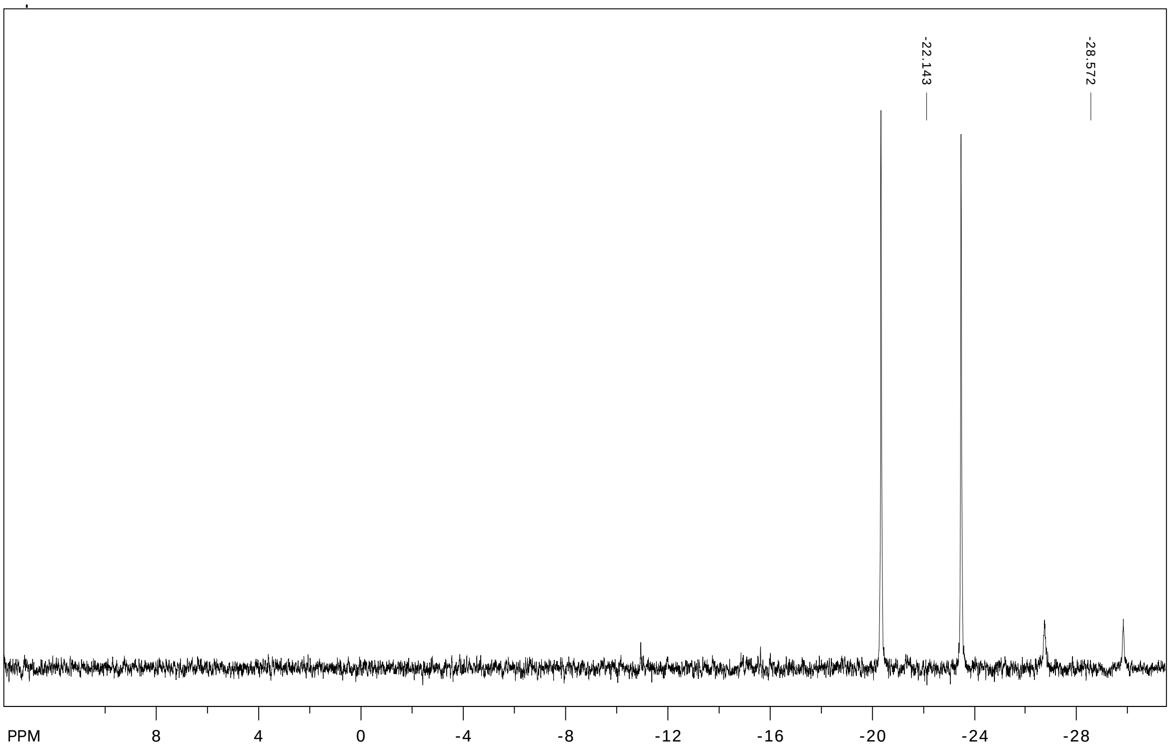

Figure S4: ^{31}P NMR spectrum of [(IPr)PPCl(IMes)]Cl (**3**) (expanded view).

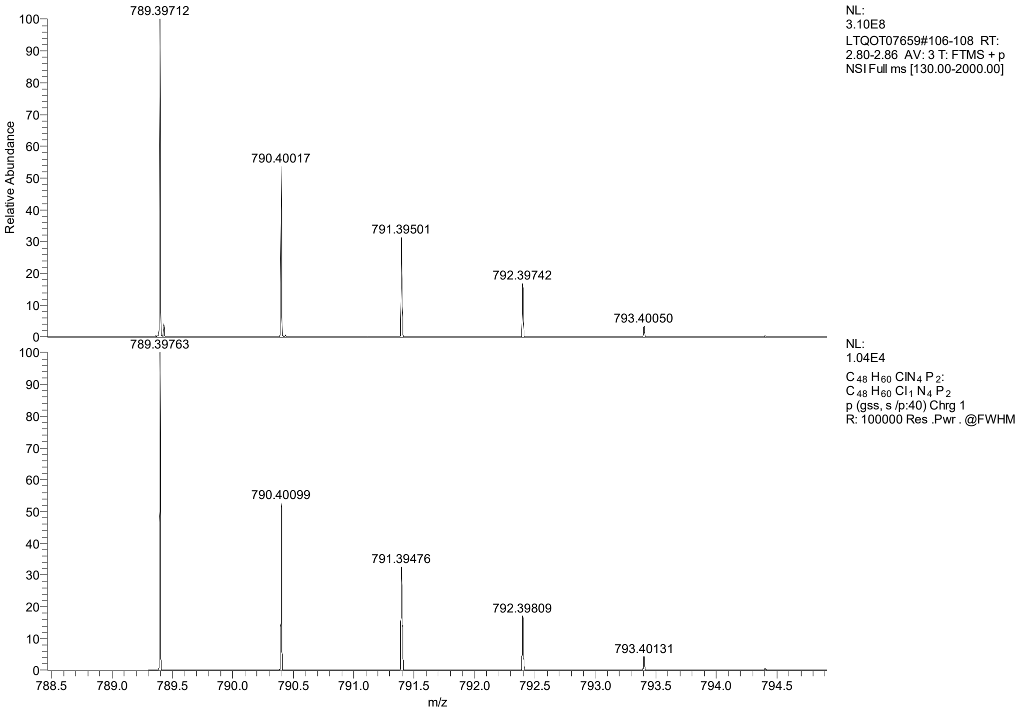

Figure S5: HRMS (in CH$_3$CN, positive ion mode) of [(IPr)PPCl(IMes)]Cl (**3**), showing the calculated and experimental mass isotopic pattern of the cationic part of the molecule.

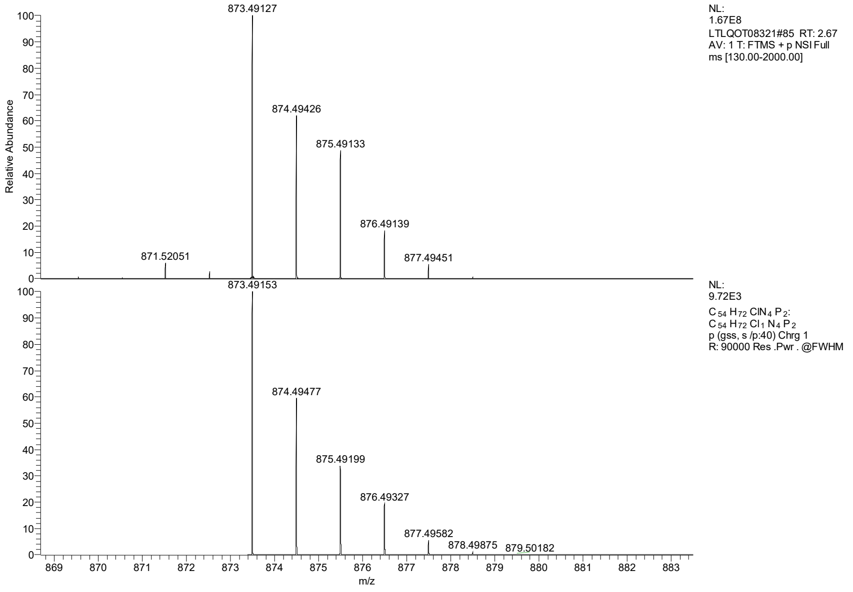

Figure S6: HRMS (CH$_3$CN, positive ion mode) of [IPr)PPCl(IPr)]Cl showing the calculated and experimental mass isotopic pattern.

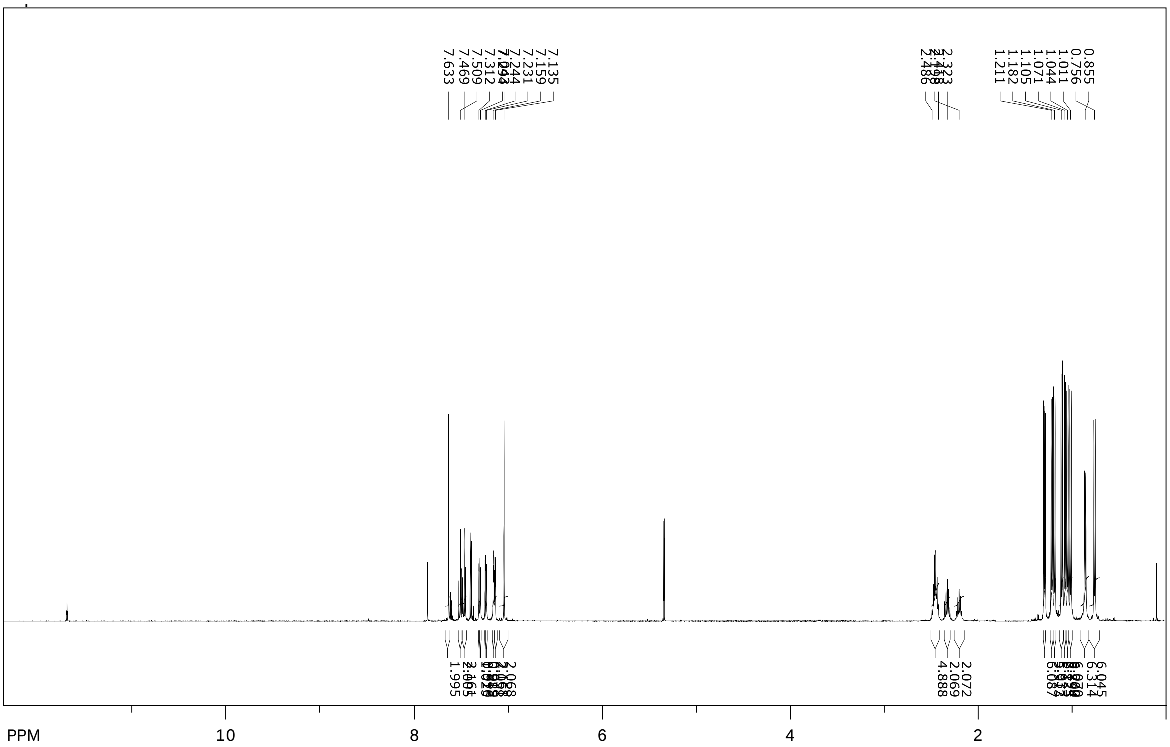

Figure S7: ^{1}H NMR spectrum of [IPr)PPCl(IPr)]Cl in CD_2Cl_2 at RT.

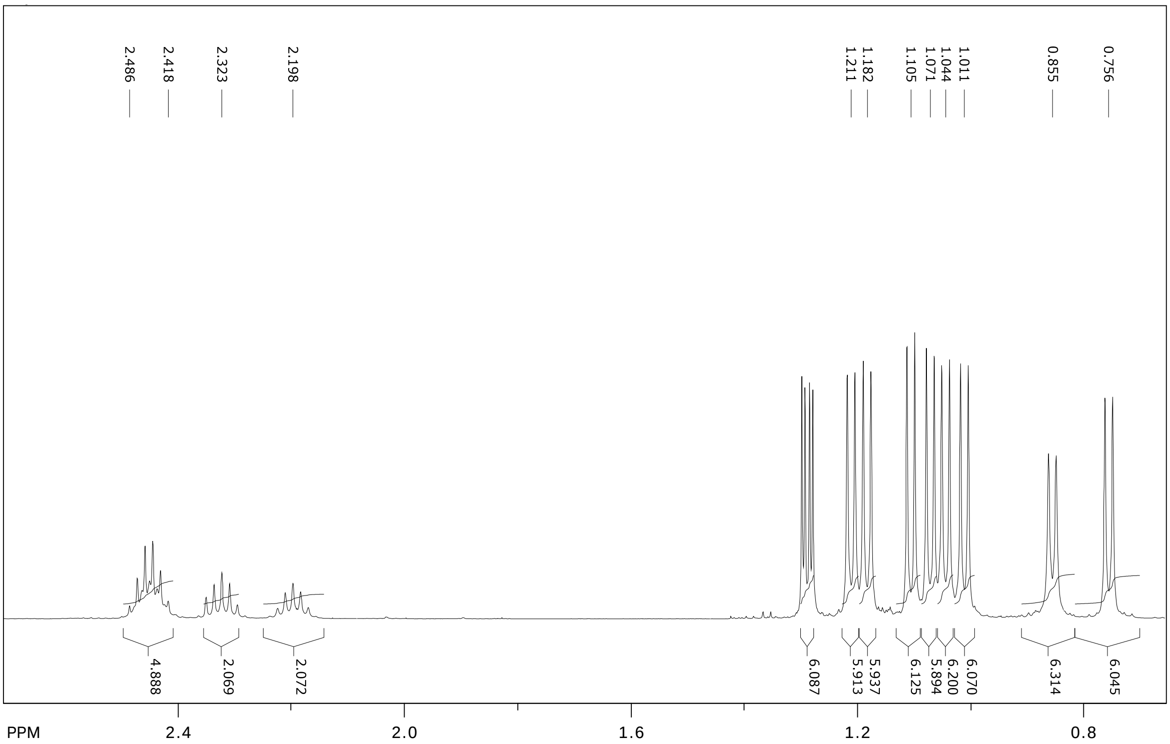

Figure S8: ^{1}H NMR spectrum of [IPr)PPCl(IPr)]Cl in CD_2Cl_2 (expanded view).

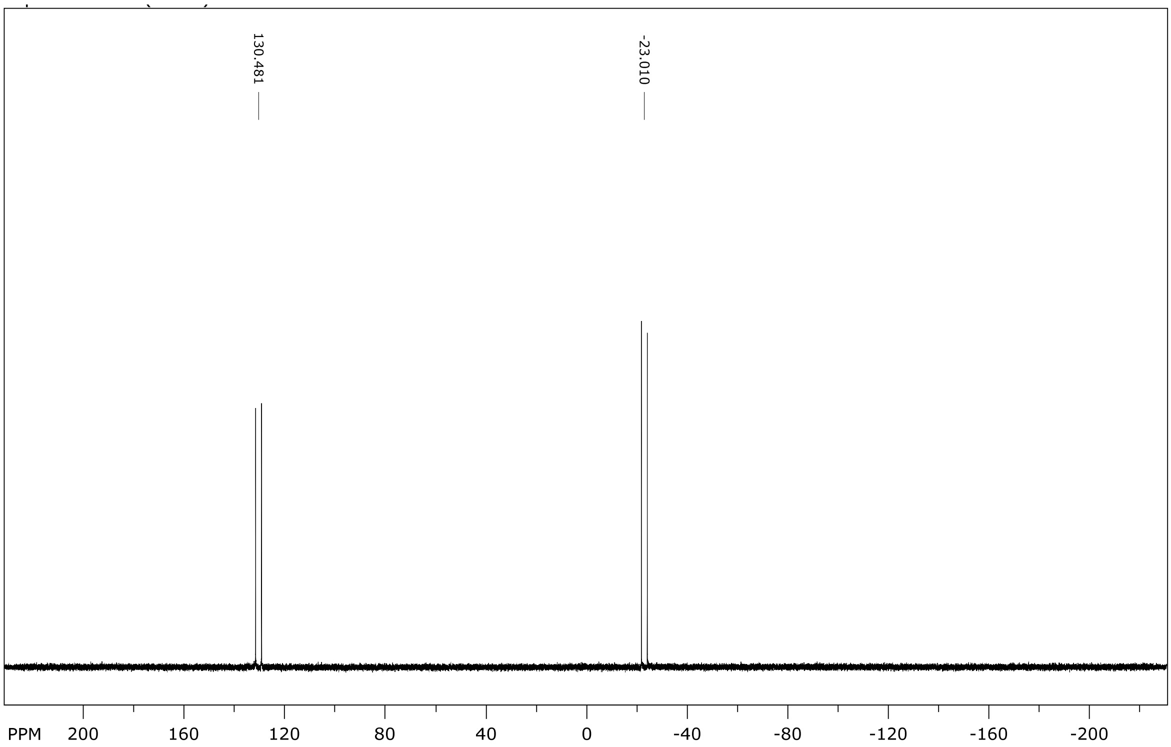

Figure S9: ^{31}P NMR spectrum of [IPr)PPCl(IPr)]Cl in CD_2Cl_2 at RT.

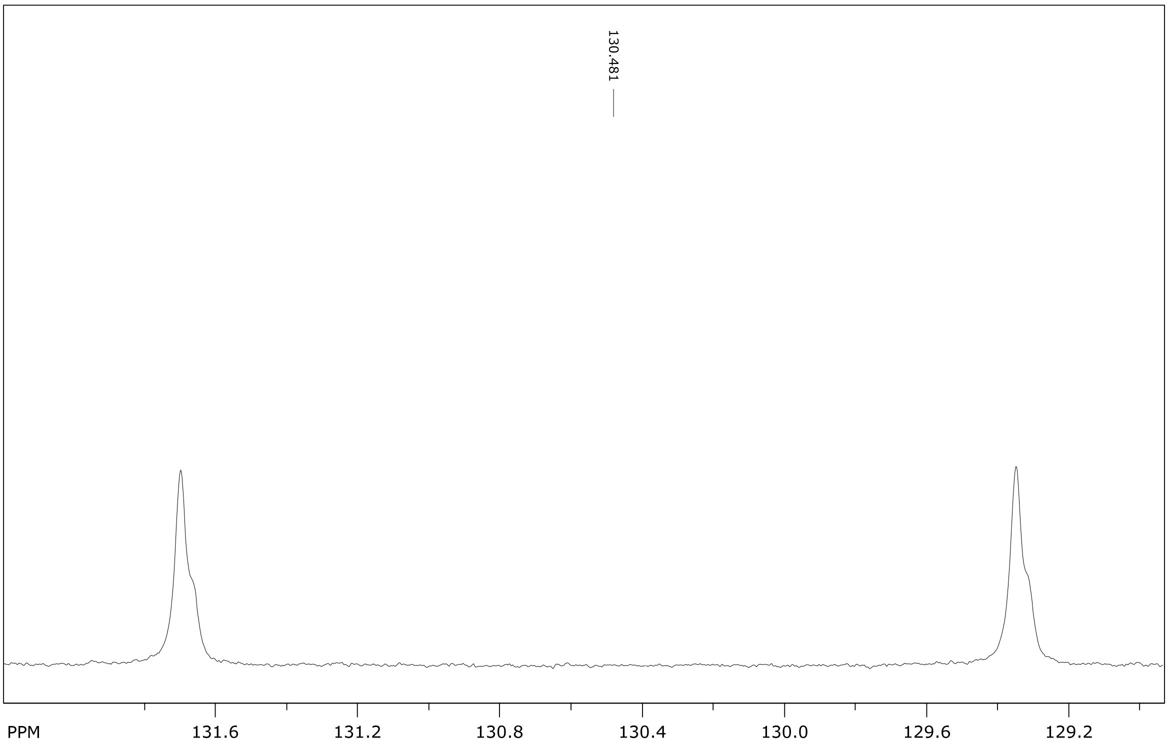

Figure S10: ^{31}P NMR spectrum of [IPr)PPCl(IPr)]Cl in CD_2Cl_2 (expanded view).

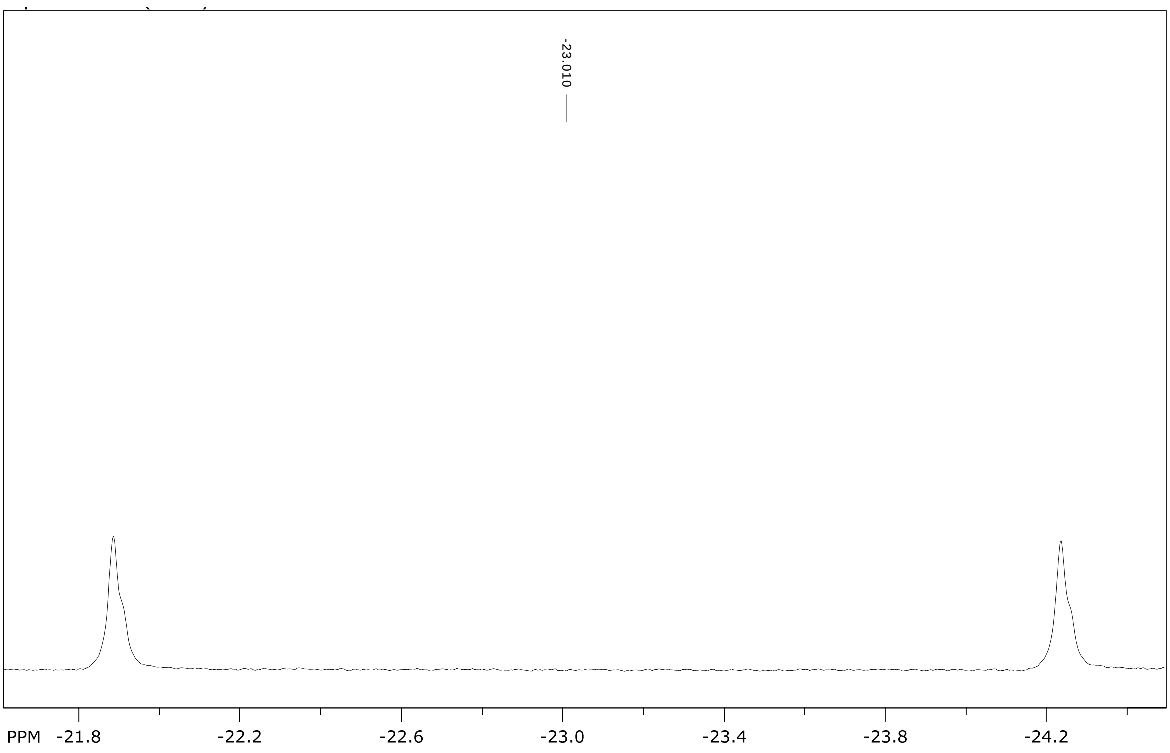

Figure S11: ^{31}P NMR spectrum of [IPr)PPCl(IPr)]Cl in CD_2Cl_2 (expanded view).

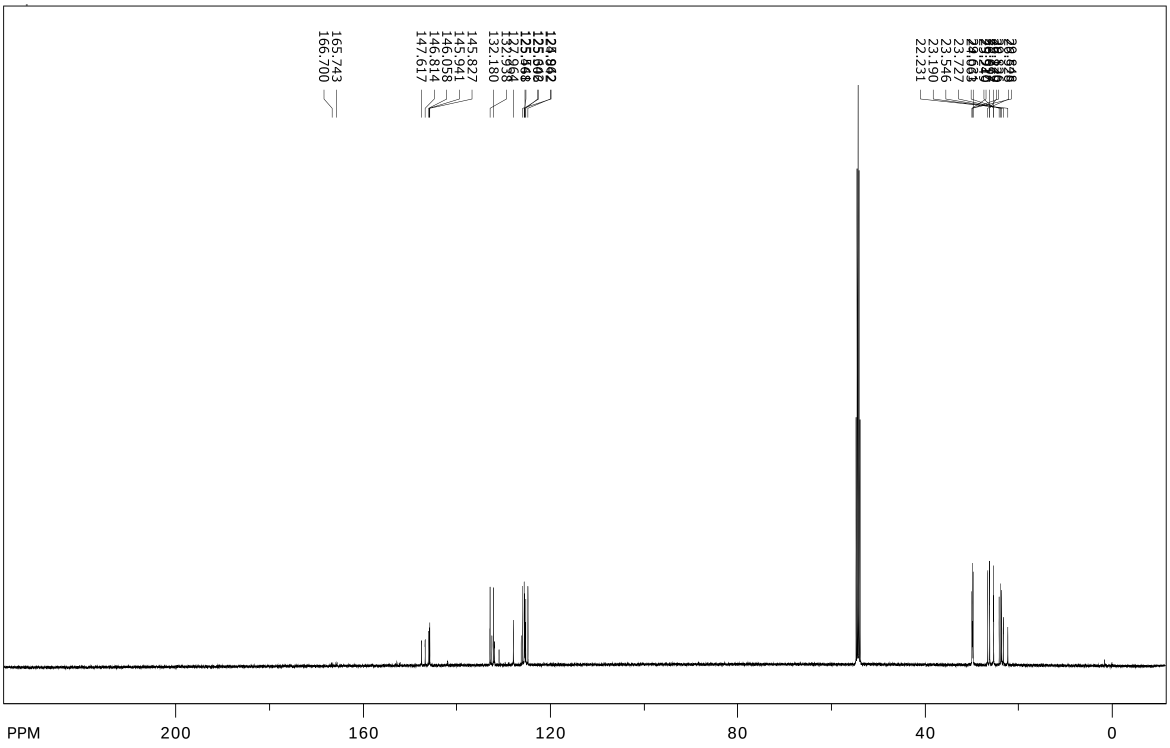

Figure S12: ^{13}C NMR spectrum of [IPr)PPCl(IPr)]Cl in CD_2Cl_2 at RT.

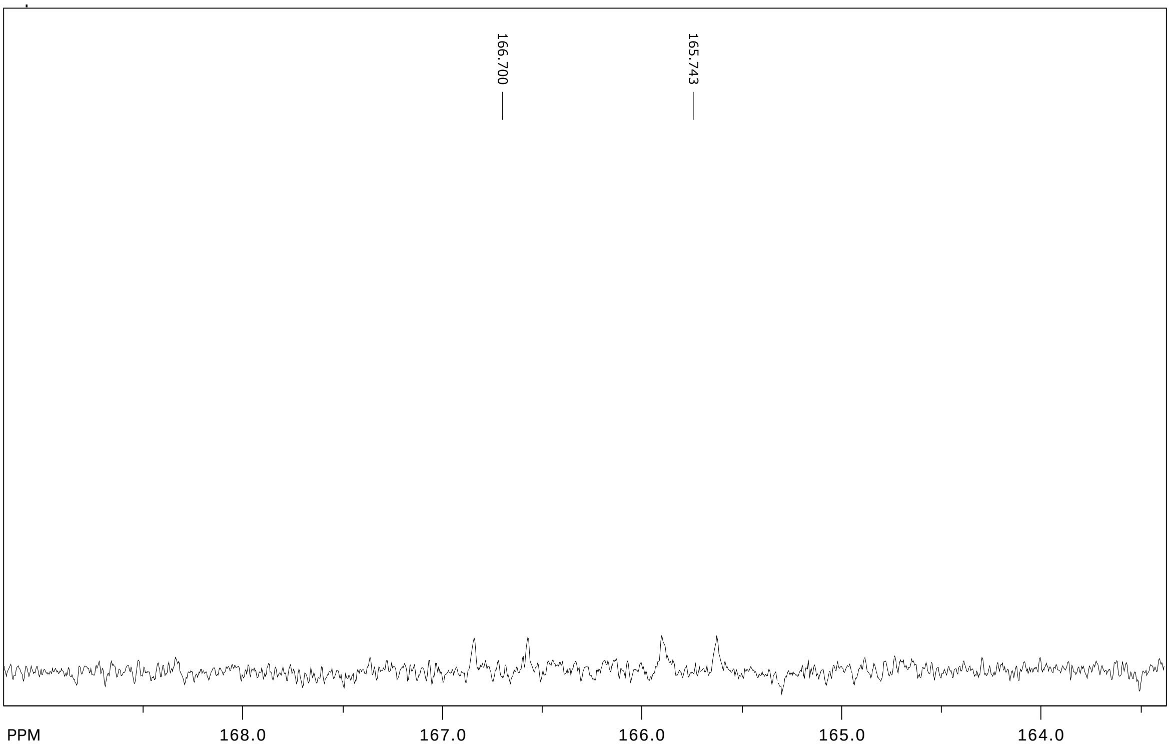

Figure S13: ^{13}C NMR spectrum of [IPr)PPCl(IPr)]Cl in CD_2Cl_2 (expanded view).

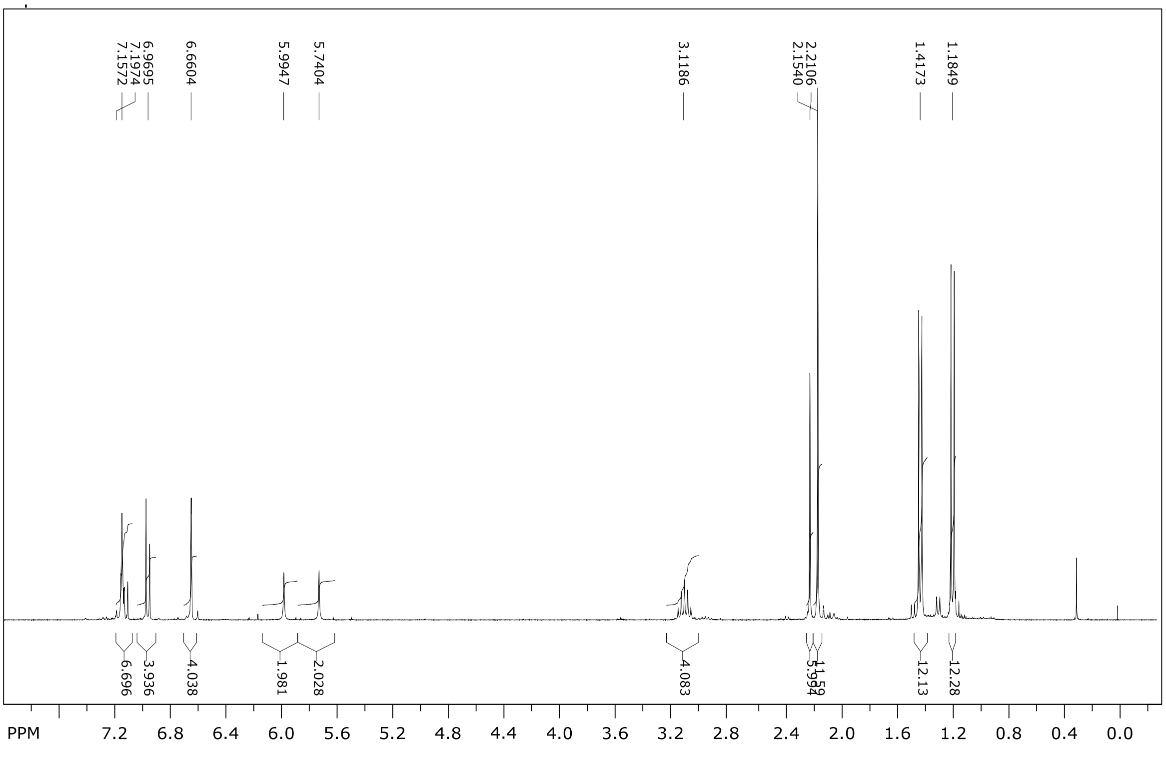

Figure S14: ^{1}H NMR spectrum of [(IPr)P–P(IMes)] (**4**) in C_6D_6 at room temperature.

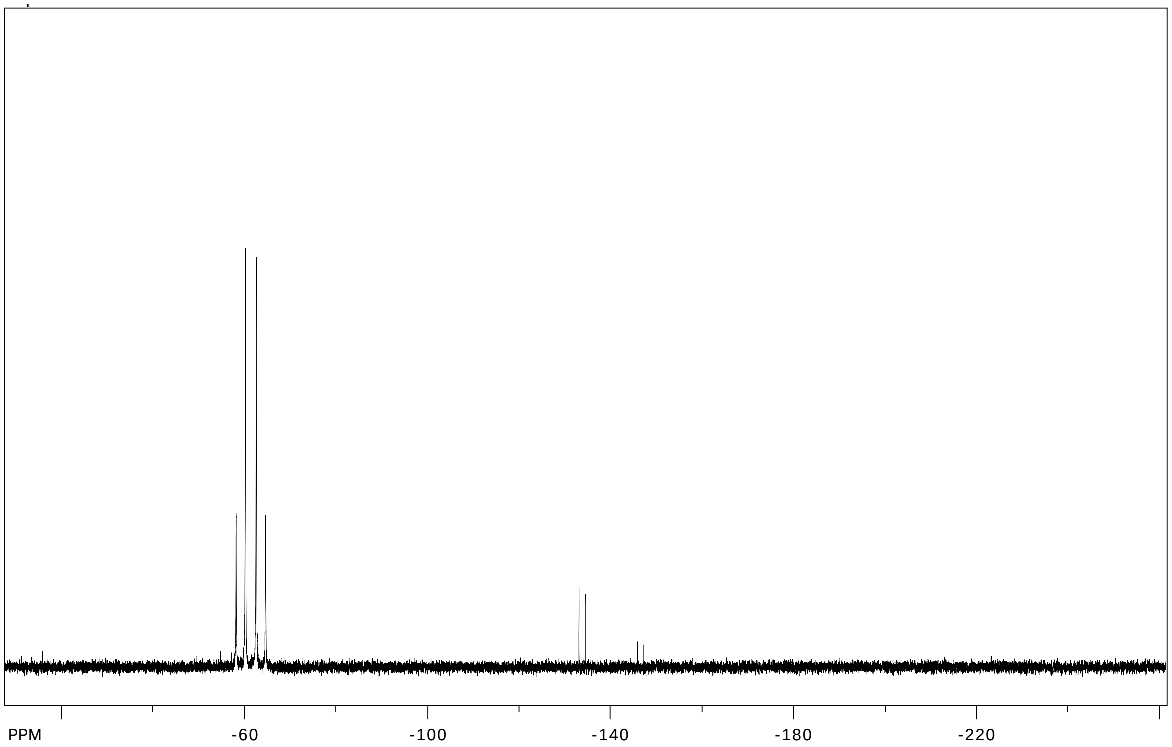

Figure S15: ^{31}P NMR spectrum of [(IPr)P–P(IMes)] (**4**) in C_6D_6 at room temperature (impurities, δ= –133.9 ppm (IPr)PH and –146.5 ppm (IMes)PH).

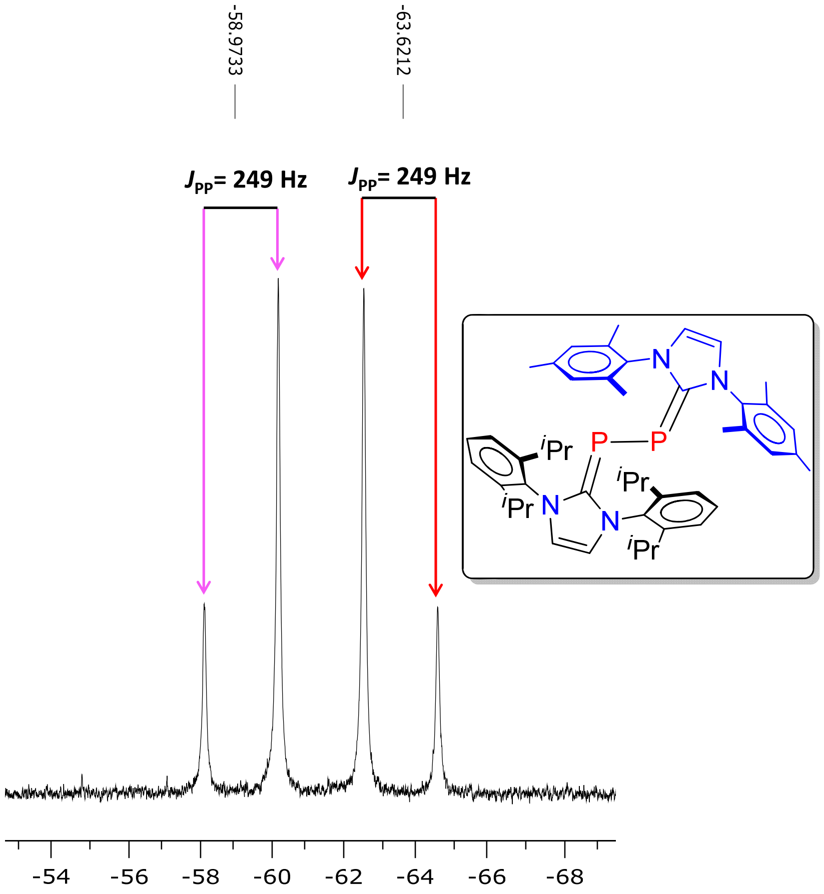

Figure S16: ^{31}P NMR spectrum of [(IPr)P–P(IMes)] (**4**) in C_6D_6 at room temperature.

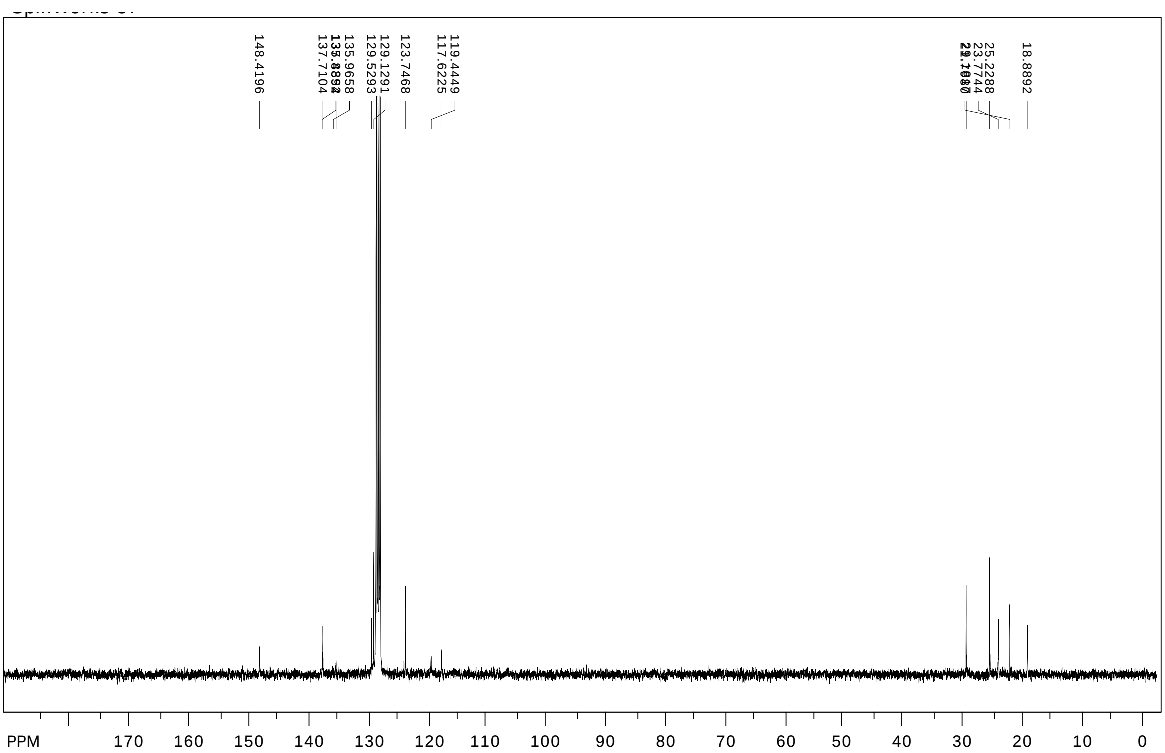

Figure S17: ^{13}C NMR spectrum of [(IPr)P–P(IMes)] (**4**) in C_6D_6 at room temperature.

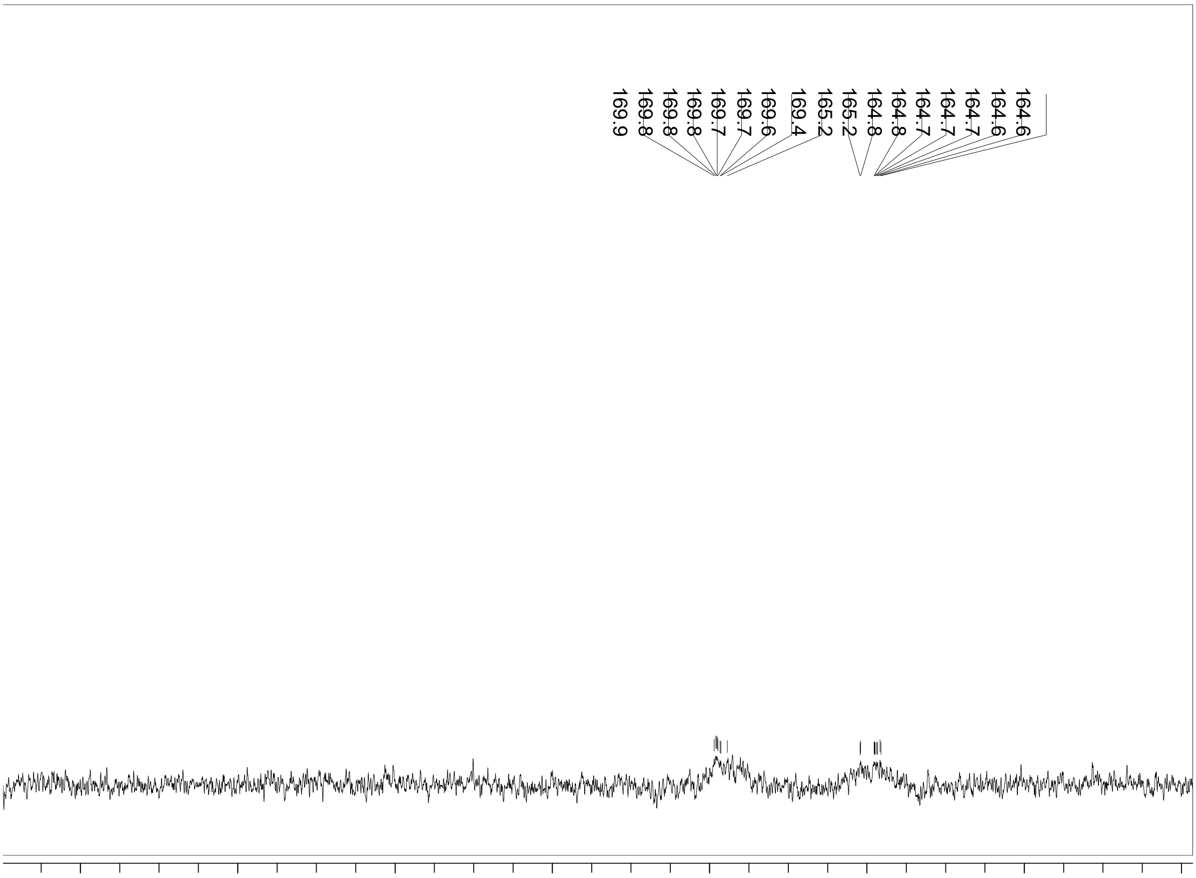

Figure S18: ^{13}C NMR spectrum of [(IPr)P–P(IMes)] (**4**) (expanded view).

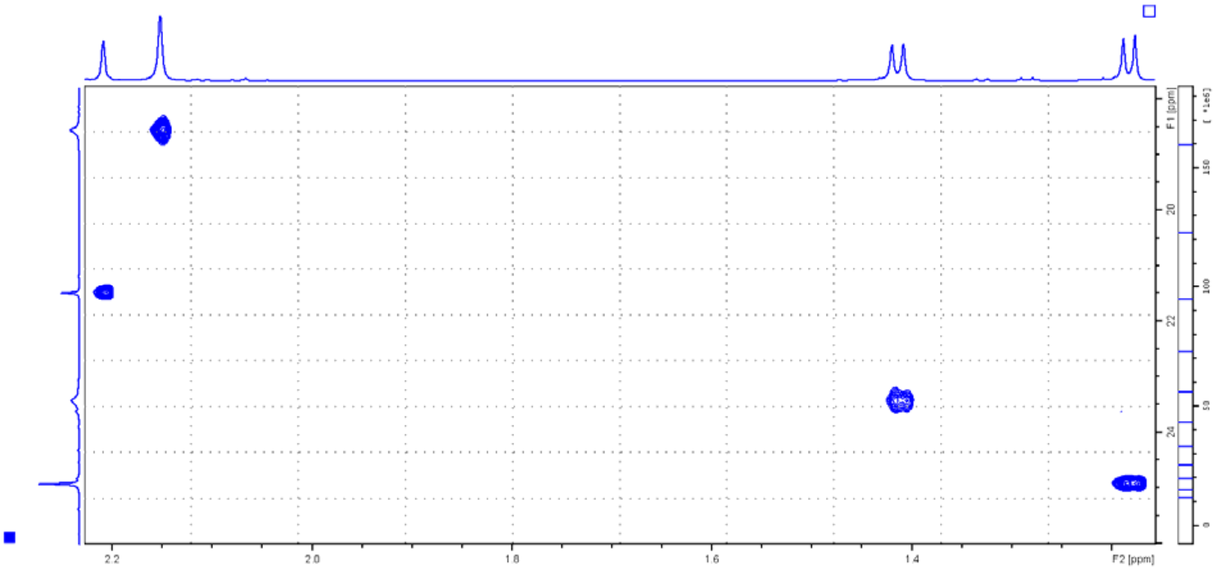

Figure S19: HSQC spectrum of [(IPr)P–P(IMes)] (**4**) (expanded view).

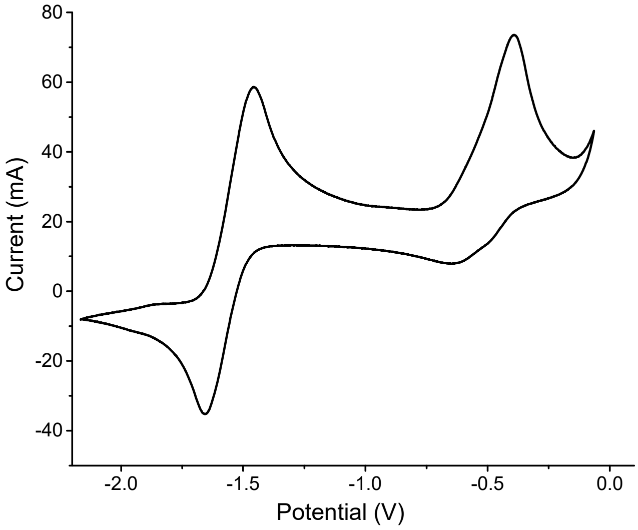

Figure S20: Cyclic voltammogram of [(IPr)P–P(IMes)] (**4**) in 10^{-3} M THF solution, 0.1 M *n*-Bu_4NPF_6, 0.1 Vs^{-1} scan rate, referenced vs. Fc^0/Fc^+ ($E_{1/2}$= –1.554, and the second at higher potential at $E_{1/2}$= –0.514 V).

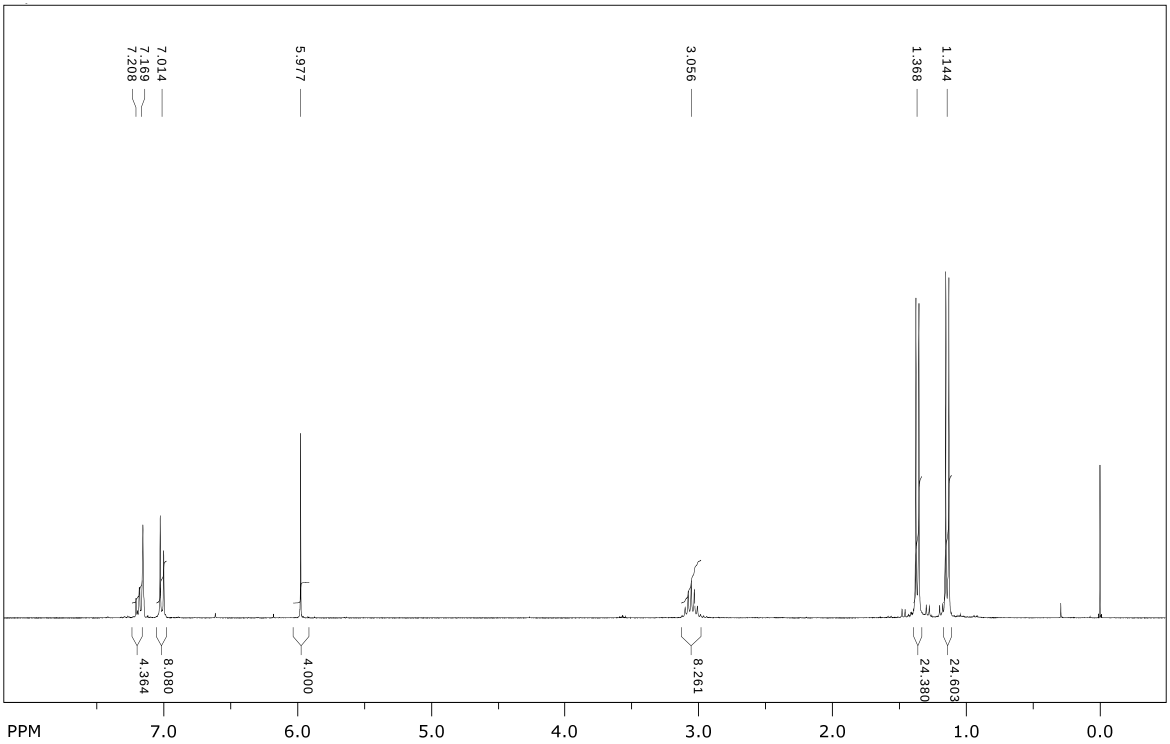

Figure S21: ^{1}H NMR spectrum of homoleptic [(IPr)PP(IPr)] (**A**) in C_6D_6.

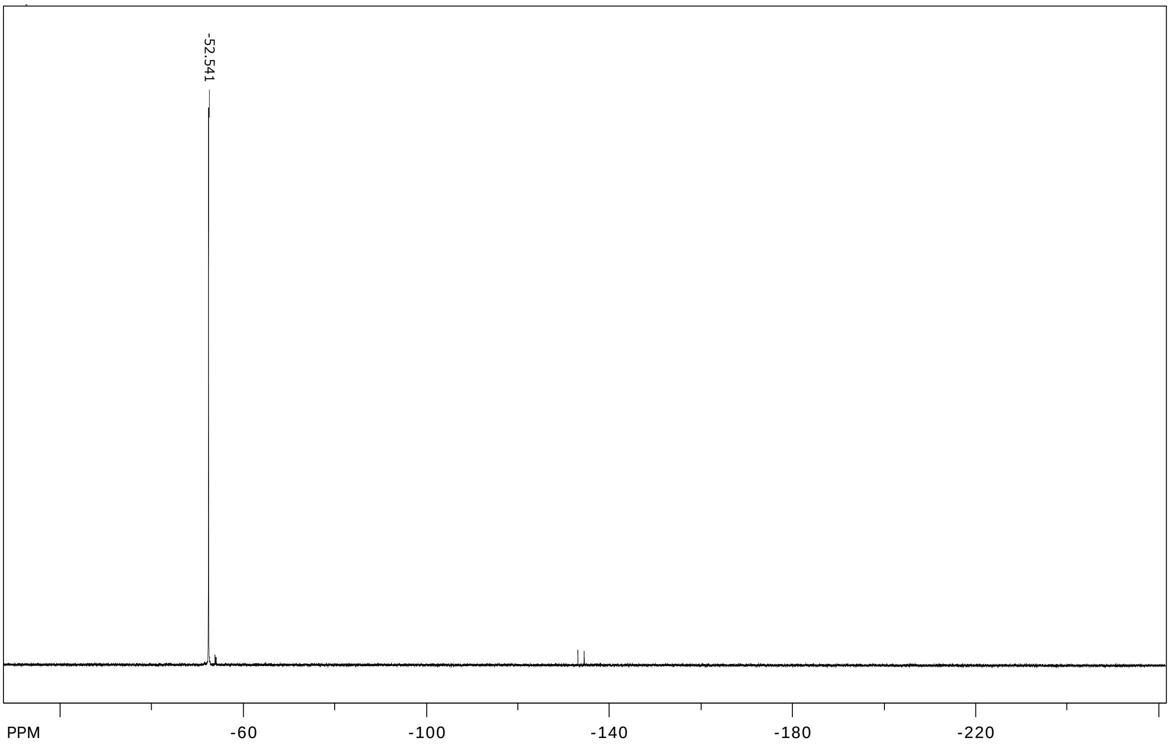

Figure S22: ^{31}P NMR spectrum of [(IPr)PP(IPr)] (**A**) in C_6D_6.

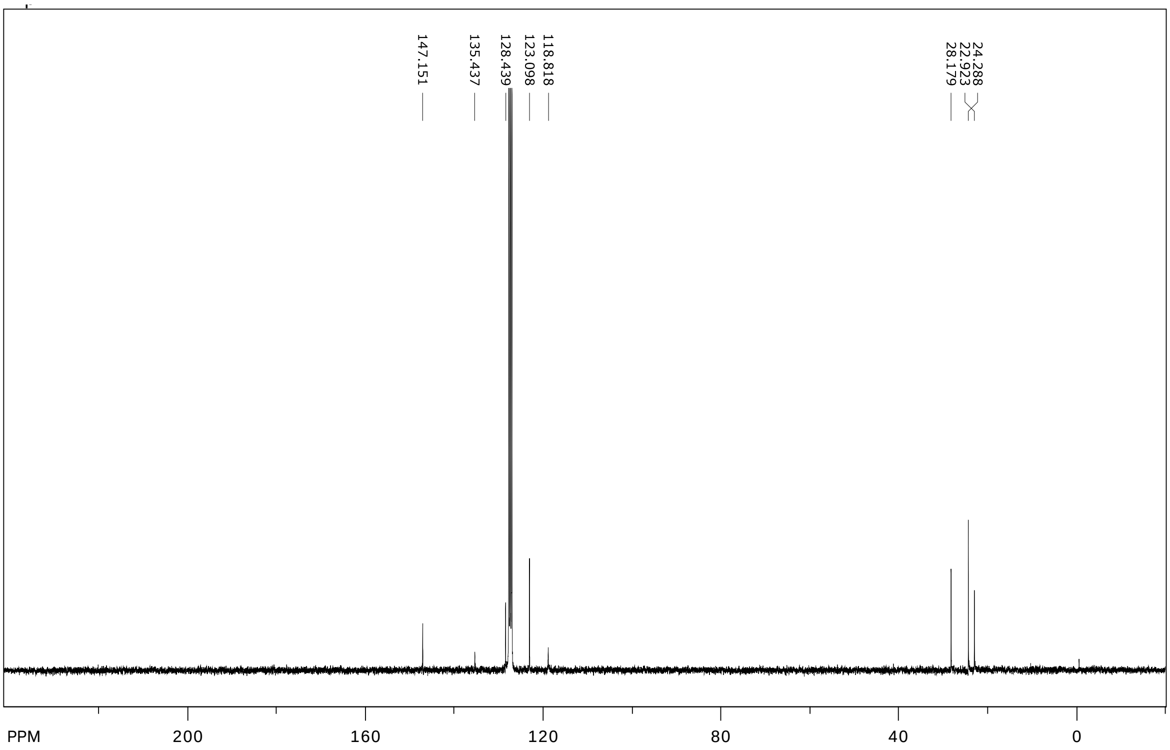

Figure S23: ^{13}C NMR spectrum of [(IPr)PP(IPr)] (**A**) in C_6D_6.

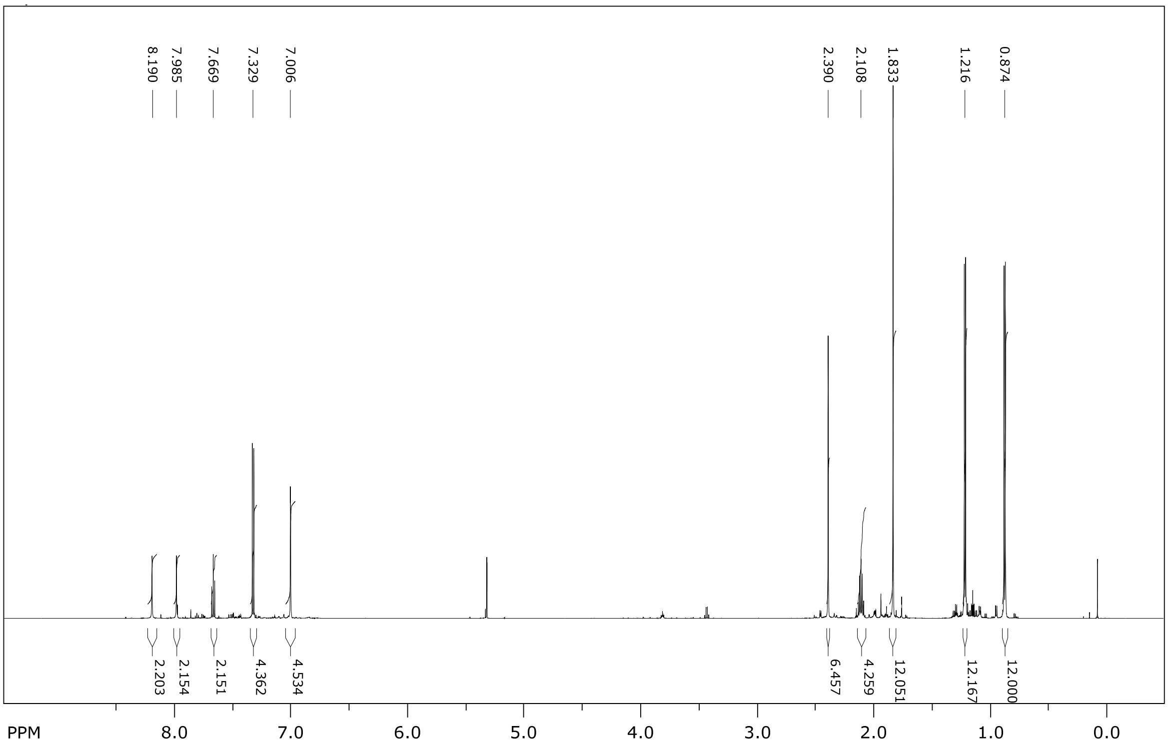

Figure S24: ^{1}H NMR spectrum of [(IPr)P=P(IMes)][GaCl$_4$]$_2$ **[6]**[GaCl$_4$]$_2$ in CD_2Cl_2 at room temperature.

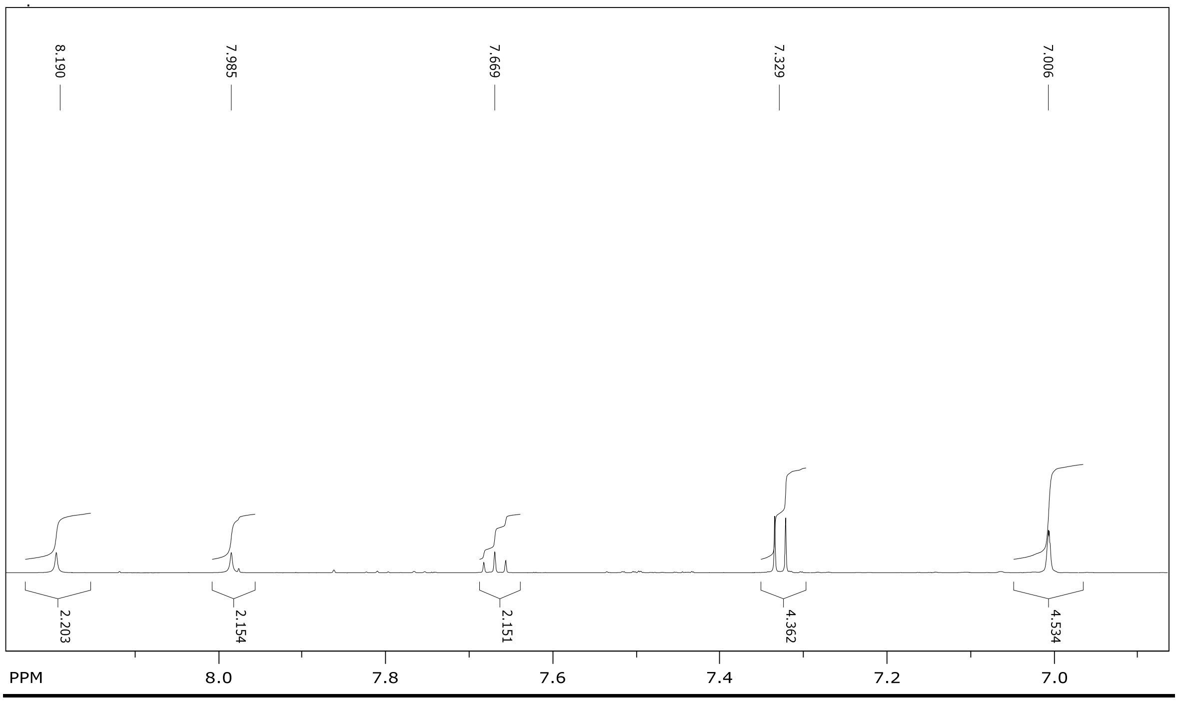

Figure S25: ^{1}H NMR spectrum (expanded view) of [(IPr)P=P(IMes)][GaCl$_4$]$_2$ **[6]**[GaCl$_4$]$_2$ in CD$_2$Cl$_2$ at room temperature.

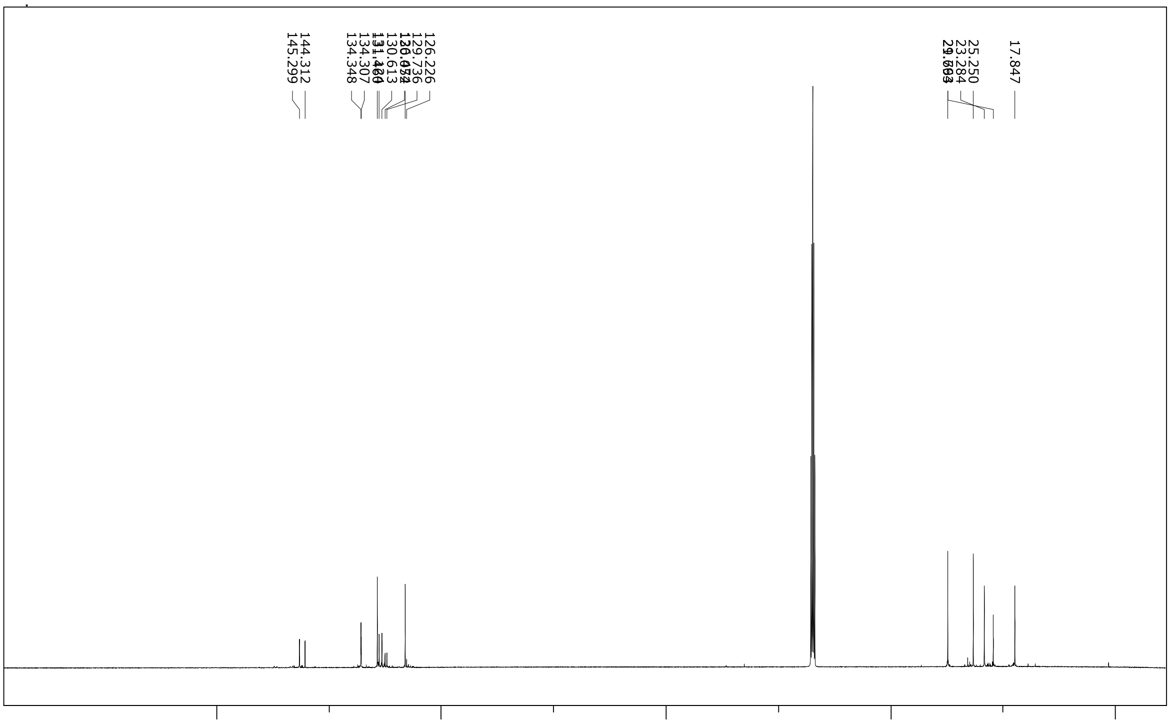

Figure S26: ^{13}C NMR spectrum of [(IPr)P=P(IMes)][GaCl$_4$]$_2$ **[6]**[GaCl$_4$]$_2$ in CD$_2$Cl$_2$ at room temperature.

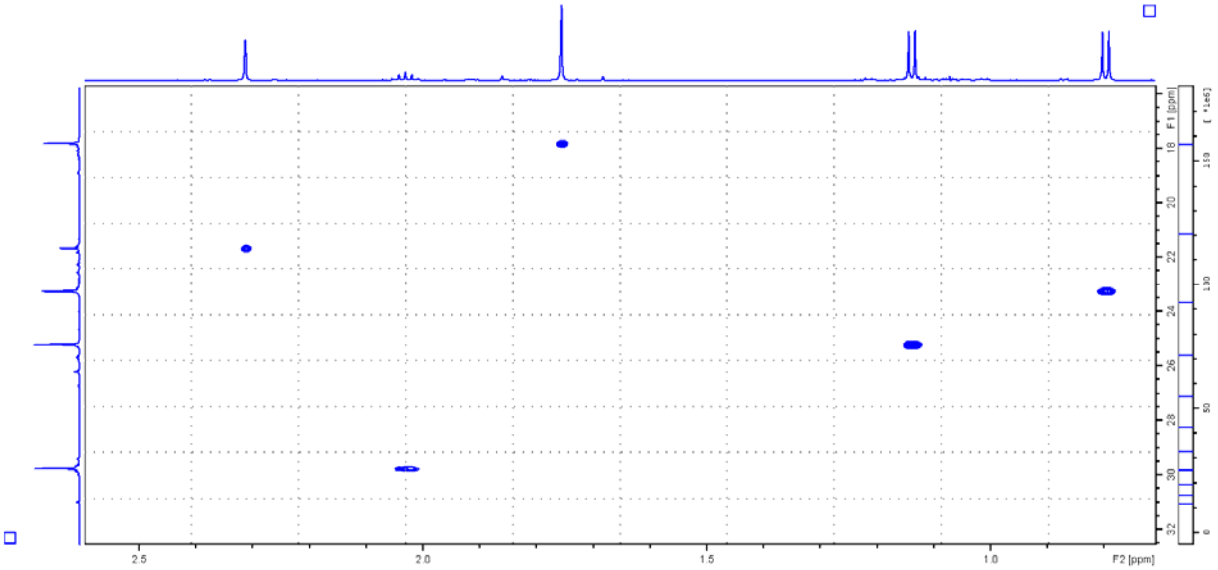

Figure S27: HSQC (expanded view) of [(IPr)P=P(IMes)][GaCl$_4$]$_2$ **[6]**[GaCl$_4$]$_2$ in CD$_2$Cl$_2$ at room temperature.

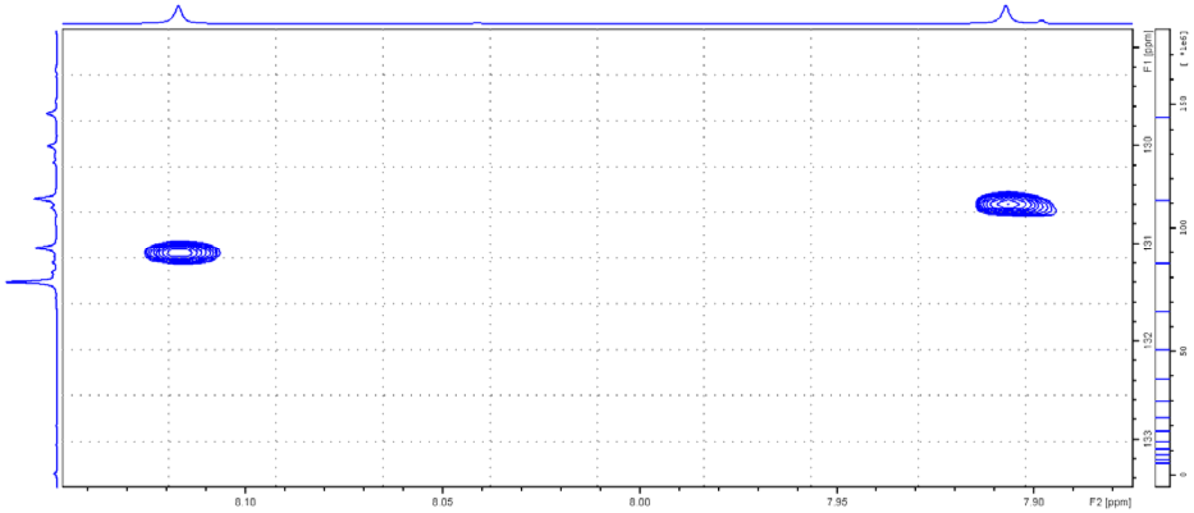

Figure S28: HSQC (expanded view) of [(IPr)P=P(IMes)][GaCl$_4$]$_2$ **[6]**[GaCl$_4$]$_2$ in CD$_2$Cl$_2$ at room temperature.

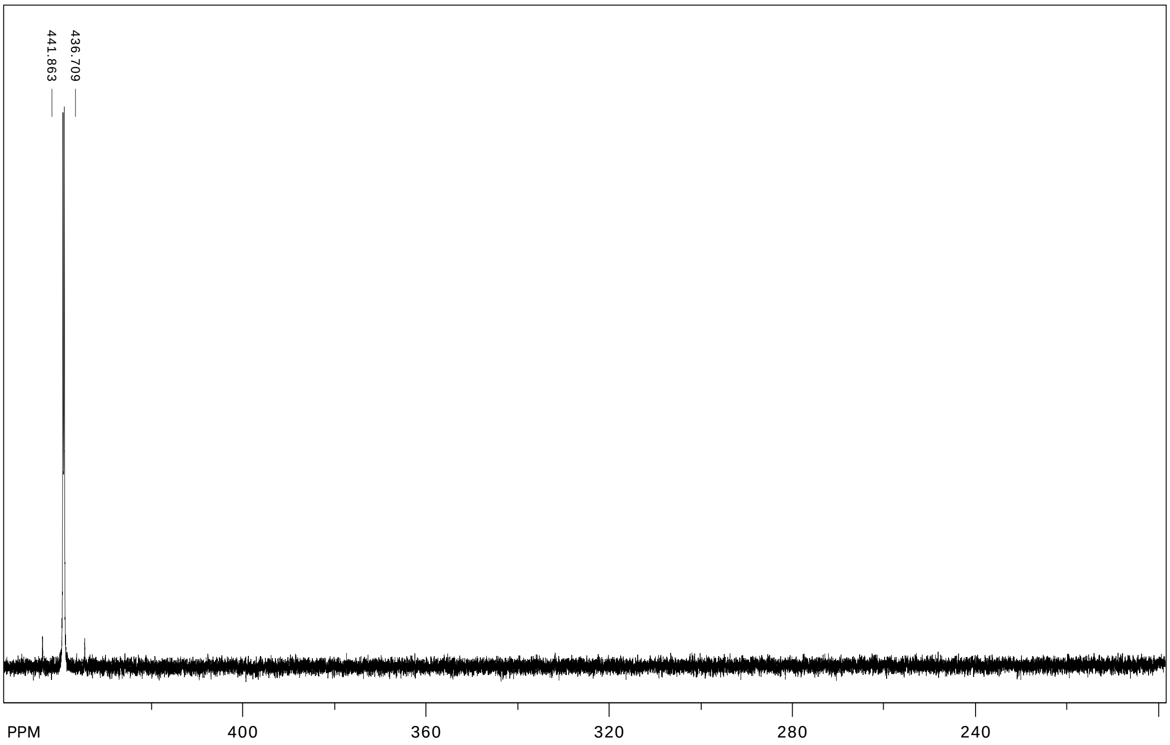

Figure S29: ^{31}P NMR spectrum of [(IPr)P=P(IMes)][GaCl$_4$]$_2$ **[6]**[GaCl$_4$]$_2$ in CD$_2$Cl$_2$ at room temperature.

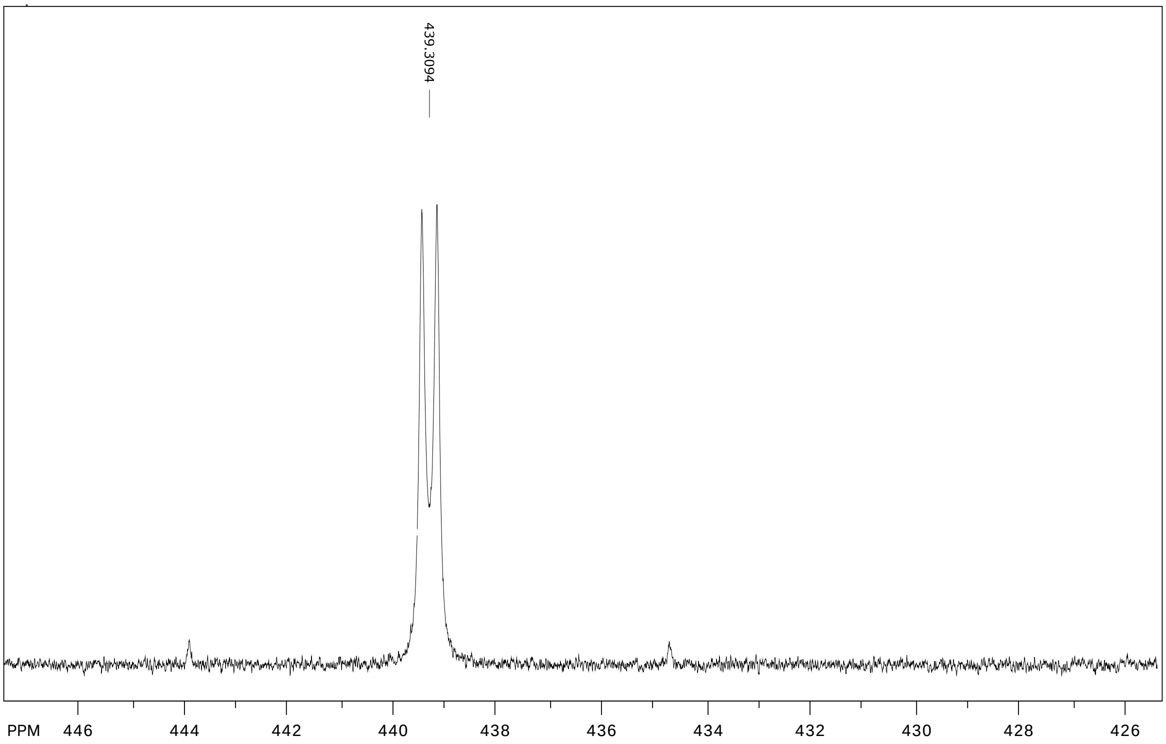

Figure S30: ^{31}P NMR spectrum of [(IPr)P=P(IMes)][GaCl$_4$]$_2$ **[6]**[GaCl$_4$]$_2$ in CD$_2$Cl$_2$ at room temperature (expanded view).

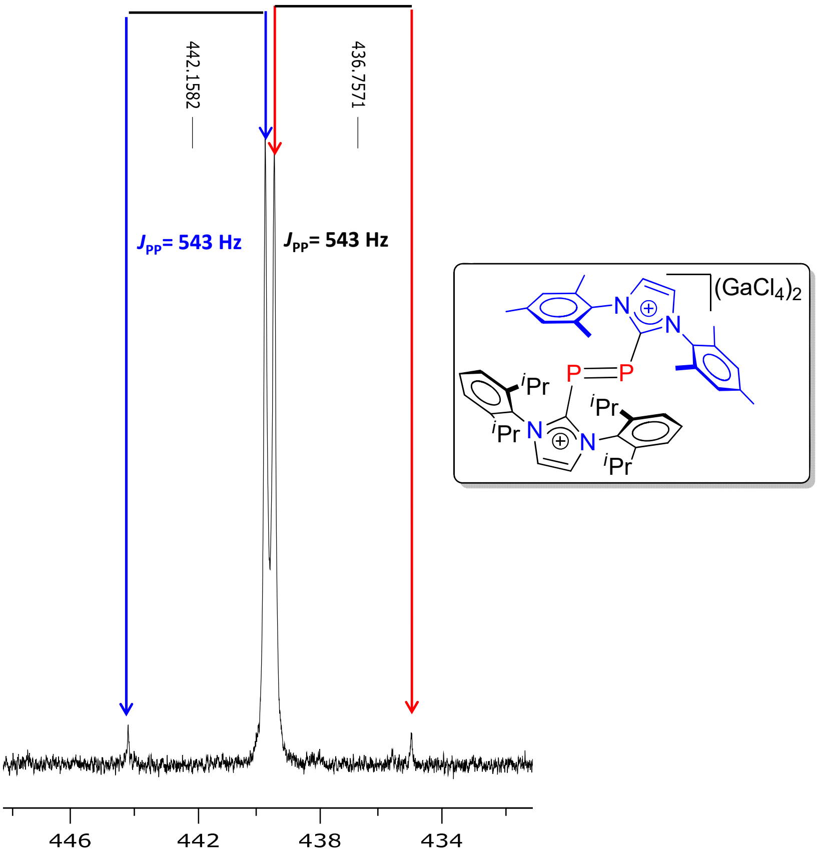

Figure S31: ^{31}P NMR spectrum of [(IPr)P=P(IMes)][GaCl$_4$]$_2$ **[6]**[GaCl$_4$]$_2$ in CD$_2$Cl$_2$ at room temperature (expanded view).

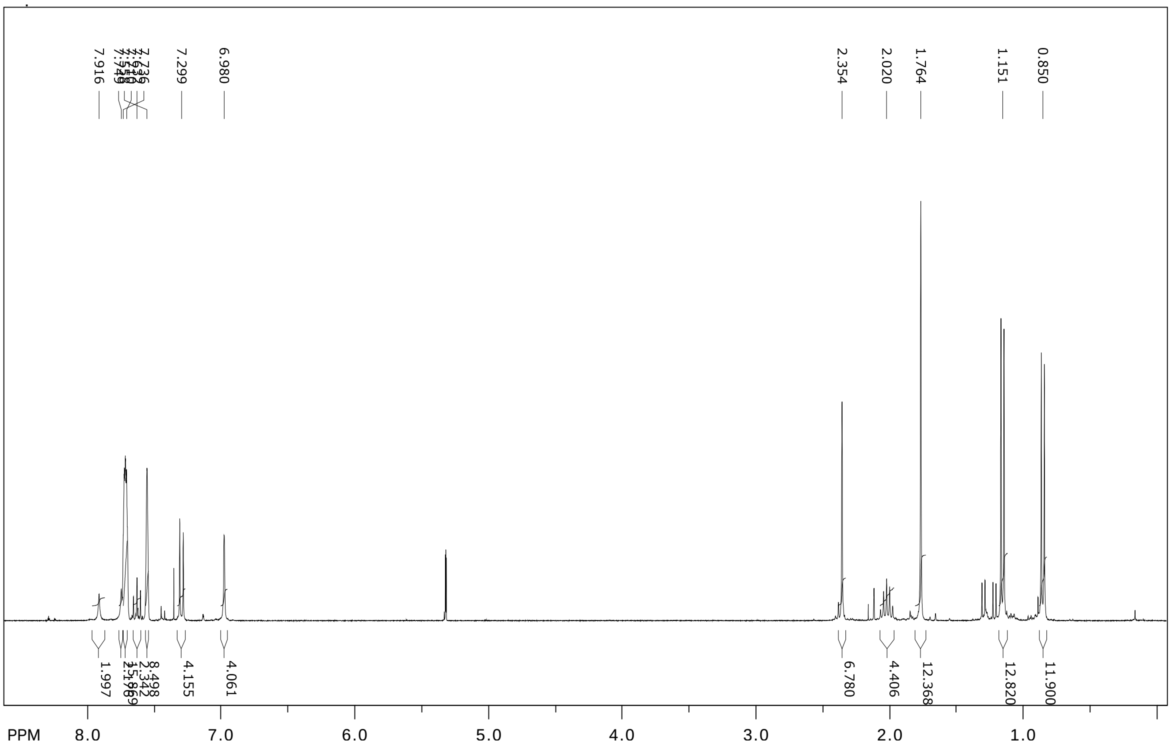

Figure S32: ^{1}H NMR spectrum of [(IPr)P=P(IMes)][BAr^F]$_2$ **[6]**[BAr^F]$_2$ in CD$_2$Cl$_2$ at room temperature.

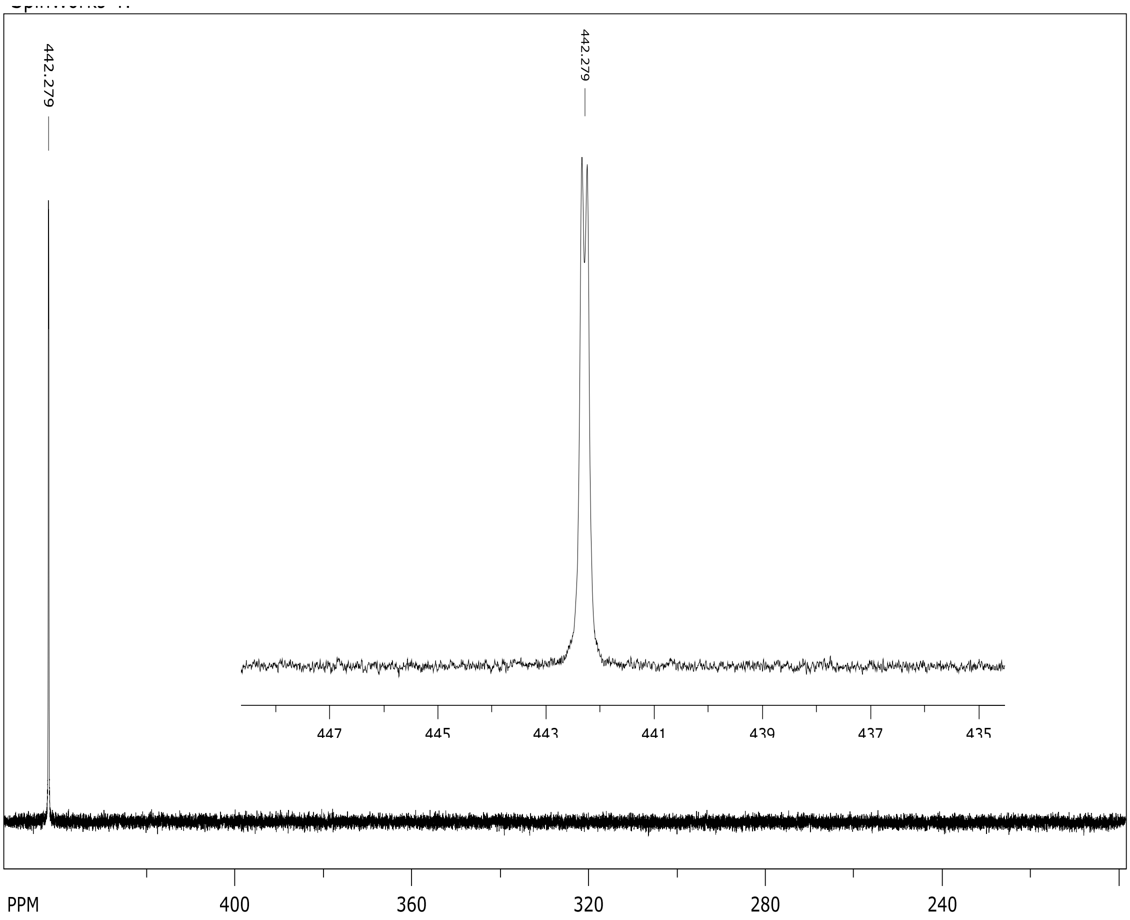

Figure S33: ^{31}P NMR spectrum of [(IPr)P=P(IMes)][BAr^F]$_2$ **[6]**[BAr^F]$_2$ in CD_2Cl_2 at room temperature (expanded view is also shown).

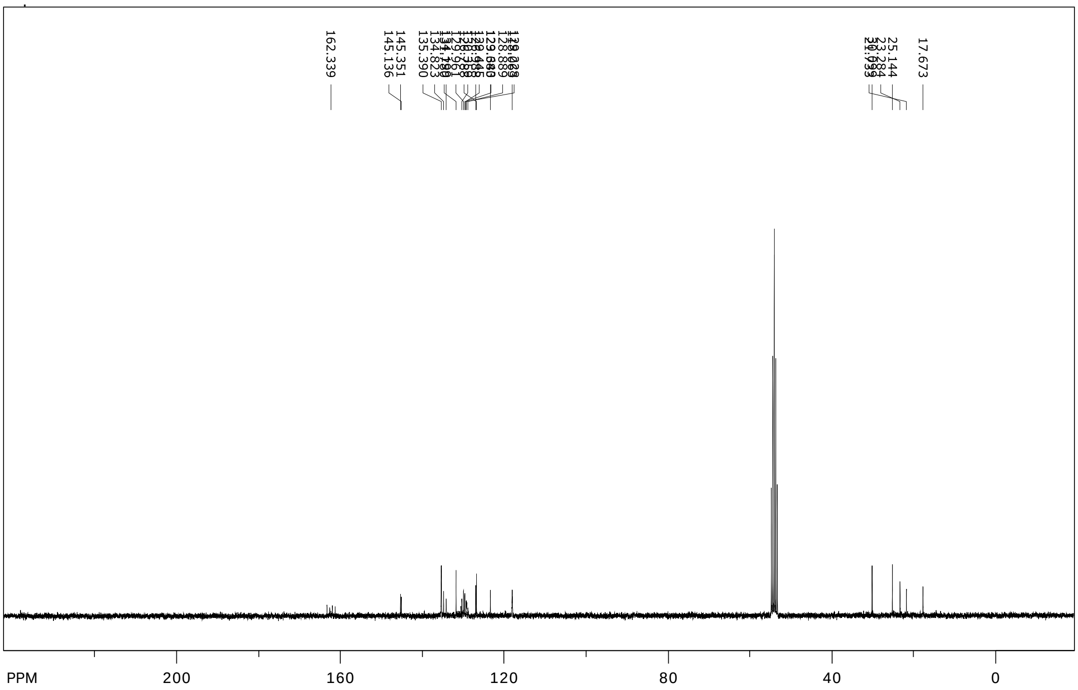

Figure S34: ^{13}C NMR spectrum of [(IPr)P=P(IMes)][BAr^F]$_2$ **[6]**[BAr^F]$_2$ in CD_2Cl_2 at room temperature.

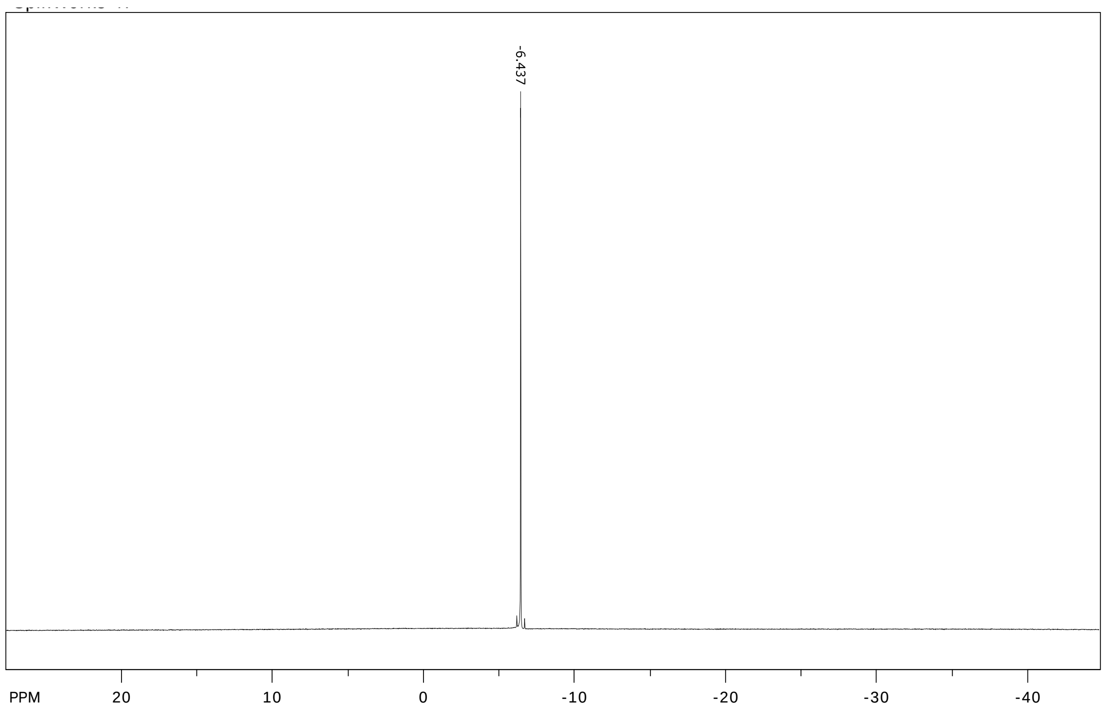

Figure S35: ^{11}B NMR spectrum of [(IPr)P=P(IMes)][BAr^F]$_2$ **[6]**[BAr^F]$_2$ in CD_2Cl_2 at room temperature.

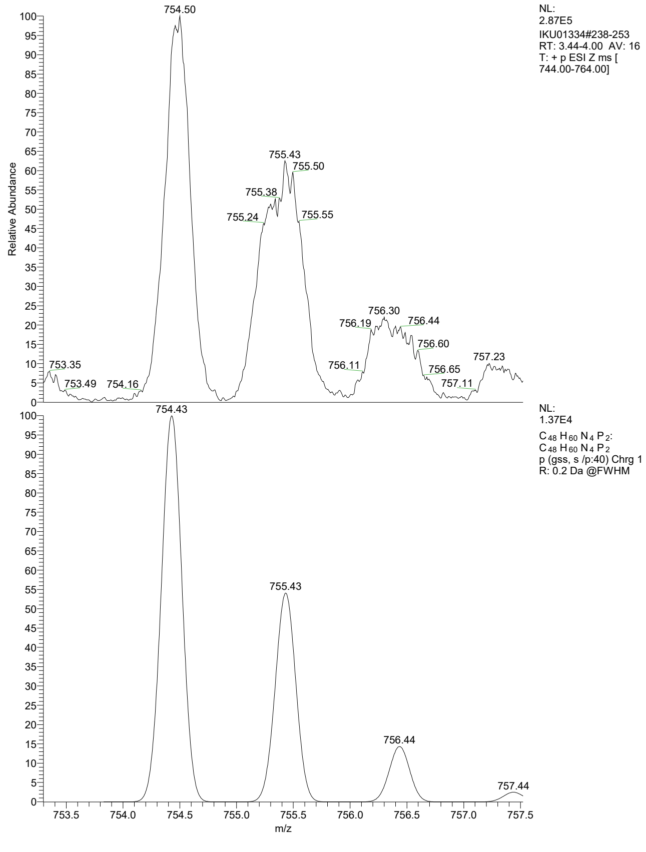

Figure S36: ESI-MS (CH_3CN, positive ion mode) of [(IPr)PP(IMes)]PF_6 **[5]**PF_6 showing the calculated and experimental mass isotopic pattern of the cationic part of the molecule.

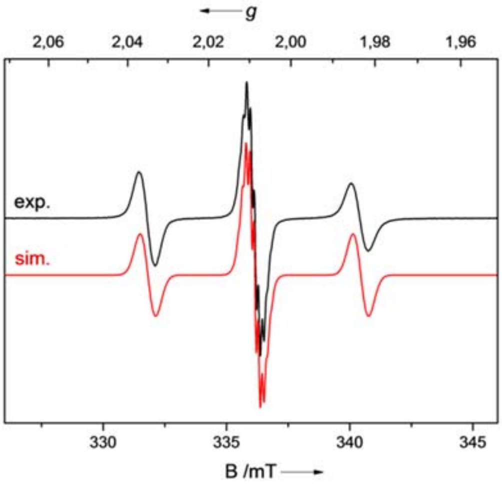

Figure S37: X-band EPR spectrum (black) and simulation (red) of the radical cation in [(IPr)PP(IMes)]PF_6, **[5]**PF_6, measured in CH_2Cl_2 at room temperature (298 K, ν = 9.450643 GHz): g_{iso}= 2.00865, $A(^{31}P)$ = 43.4 G.

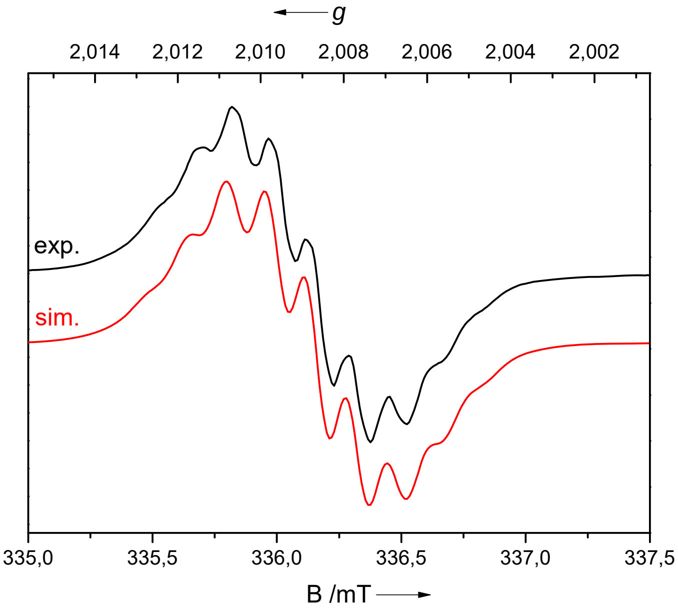

Figure S38: Expanded X-band EPR spectrum (black) and simulation (red) of the radical cation in [(IPr)PP(IMes)]PF_6, **[5]**PF_6, measured in CH_2Cl_2 (298 K, ν = 9.450643 GHz): g_{iso} = 2.00865, hyperfine coupling with the four ^{14}N-nuclei ($A(^{14}N)$ = 1.6 G).

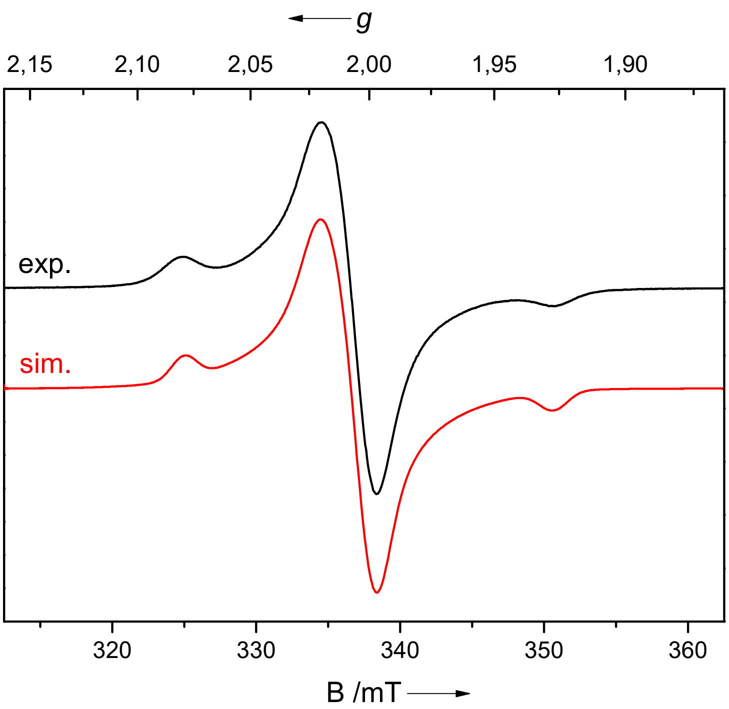

Figure S39: Rhombic X-band EPR spectrum (black) and simulation (red) of the radical cation in [(IPr)PP(IMes)]PF_6, **[5]**PF_6, measured in frozen CH_2Cl_2 (8 K, ν = 9.456944 GHz): g_x = 1.92858, g_y = 2.00358, g_z = 2.08088.

C) X-ray Crystallographic Data

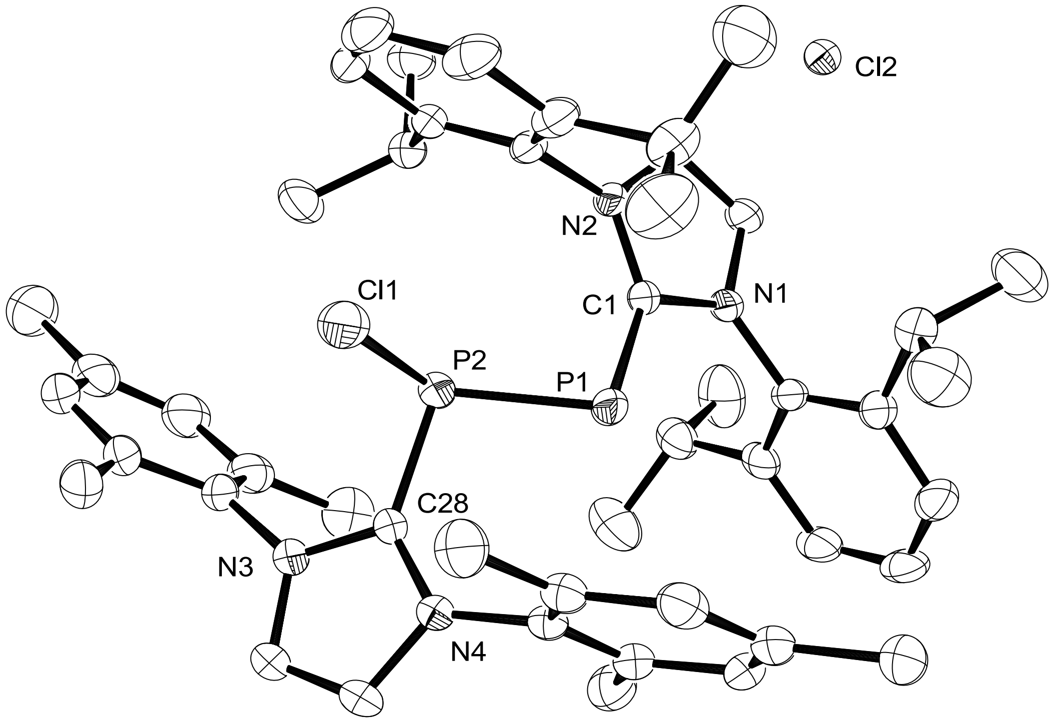

Figure S40: ORTEP diagram of **3** with thermal displacement parameters drawn at 50% probability level. Hydrogen atoms and solvent molecules are omitted for clarity. Selected bond lengths [Å] and angles [°]: P1–P2 2.1067(10), P2–Cl1 2.1560(11), C1–P1 1.817(3), C28-P2 1.851(3), N4-C28-N3 106.2(2), N2-C1-N1 105.8(2), C1-P1-P2 94.99(9), C28-P2-P 99.89(9).

Table S1: Crystal data and structure refinement for **3**·3CH_2Cl_2

CCDC	1572769	
Sum formula	$C_{51}H_{66}Cl_8N_4P_2$	
Moiety formula	$C_{48}H_{60}$ Cl_2 N_4 P_2, Cl, 3(CH_2Cl_2)	
Formula weight	1080.61	
Temperature	100(2) K	
Wavelength	1.54184 Å	
Instrument (scan mode)	Oxford Diffraction, Xcalibur, Atlas, Nova ω scan)	
Crystal system, Space group	Triclinic, $P\overline{1}$ (no. 2)	
Unit cell dimensions	a = 11.2720(8) Å	α= 94.872(5)°.
	b = 15.0620(10) Å	β= 91.976(5)°.
	c = 16.43380(10) Å	γ = 93.136(5)°.
Volume, Z	2773.7(3) Å^3, 2	
Cell determination	17941 refl., 3.79° <= θ <= 76.13°	
Density (calculated)	1.294 Mg/m^3	
Absorption coefficient	4.543 mm^{-1}	
F(000)	1132	
Crystal habitus	flake (clear dark green)	

Crystal size	0.15 x 0.05 x 0.01 mm^3
Data collection	3.823° < θ < 76.318°
Completeness to θ = 67.684°	100.0 %
Index ranges	-14 <= h <= 14, -18 <= k <= 18, -20 <= l <= 19
Reflections collected / indep. / obs.	64014 / 11513 (Rint = 0.0737) / 9141
Absorption correction	Semi-empirical from equivalents
Max. and min. transmission	1.00000 and 0.72545
Solution method	iterative methods
Refinement method	Full-matrix least-squares on F^2
Hydrogen solution / refinement	geom / constr
Data / restraints / parameters	11513 / 0 / 628
Goodness-of-fit on F^2	1.028
Final R indices [I>2σ(I)]	R1 = 0.0558, wR2 = 0.1472
R indices (all data)	R1 = 0.0713, wR2 = 0.1595
Largest diff. peak and hole	1.249 and -0.997 e.Å^{-3}
Weighting scheme	$w=1/[\sigma^2(Fo^2)+(0.0801P)^2+2.5541P]$ where $P=(Fo^2+2Fc^2)/3$

Measurement and Refinement Details: A disordered molecule of dichloromethane was refined using a split atom model (0.535(7) SOF of main component).

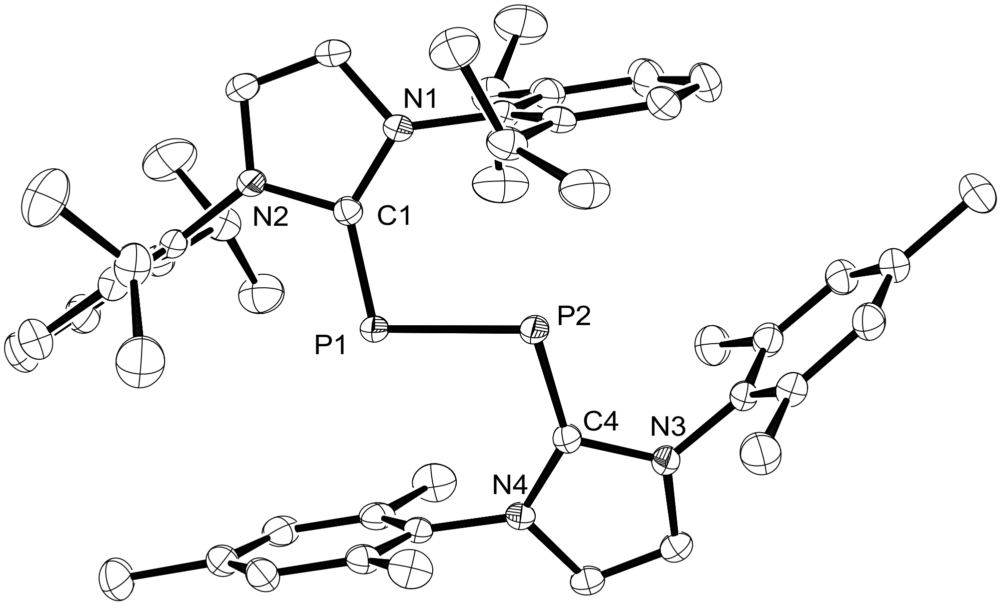

Figure S41: ORTEP diagram of [(IPr)P–P(IMes)] **4** with thermal displacement parameters drawn at 50 % probability level. Hydrogen atoms are omitted for clarity. Selected bond lengths [Å] and angles [°]: P1–P2 2.1897(4), C1–P1 1.7502(11), C4–P2 1.7488(11), N4-C4-N3 103.55(9), C1-P1-P2 101.50(4), C4-P2-P2 102.54(4).

Table S2: Crystal data and structure refinement for **4**

CCDC number	1572770	
Empirical formula	$C_{48}H_{60}N_4P_2$	
Formula weight	754.94	
Temperature	100(2) K	
Wavelength	1.54184 Å	
Instrument (scan mode)	Oxford Diffraction Xcalibur, Atlas, Nova (ω scan)	
Crystal system	Triclinic	
Space group	$P\bar{1}$	
Unit cell dimensions	a = 10.7604(2) Å	α = 100.342(2)°
	b = 12.9388(4) Å	β = 104.409(2)°
	c = 18.3755(6) Å	γ = 110.565(2)°
Volume	2217.19(11) Å^3	
Z	2	
Density (calculated)	1.131 Mg/m^3	
Absorption coefficient	1.155 mm^{-1}	
F(000)	812	
Crystal habitus	block (red)	
Crystal size	0.240 x 0.200 x 0.140 mm^3	
Theta range for data collection	3.818 to 76.107°	
Index ranges	-13<=h<=13, -16<=k<=16, -23<=l<=23	
Reflections collected	94739	
Independent reflections	9240 [R(int) = 0.0375]	
Completeness to θ = 67.684°	100.0 %	
Absorption correction	Gaussian	
Max. and min. transmission	0.938 and 0.889	
Refinement method	Full-matrix least-squares on F^2	
Data / restraints / parameters	9240 / 0 / 501	
Goodness-of-fit on F^2	1.036	
Final R indices [I>2σ(I)]	R1 = 0.0362, wR2 = 0.0948	
R indices (all data)	R1 = 0.0386, wR2 = 0.0971	
Extinction coefficient	n/a	
Largest diff. peak and hole	0.209 and -0.363 e.Å^{-3}	
Crystallization Details:	*n*-hexane (saturated solution)	
Measurement and Refinement Details:	The hydrogen atoms of the methyl group on C27 were refined over two positions (HFIX127).	

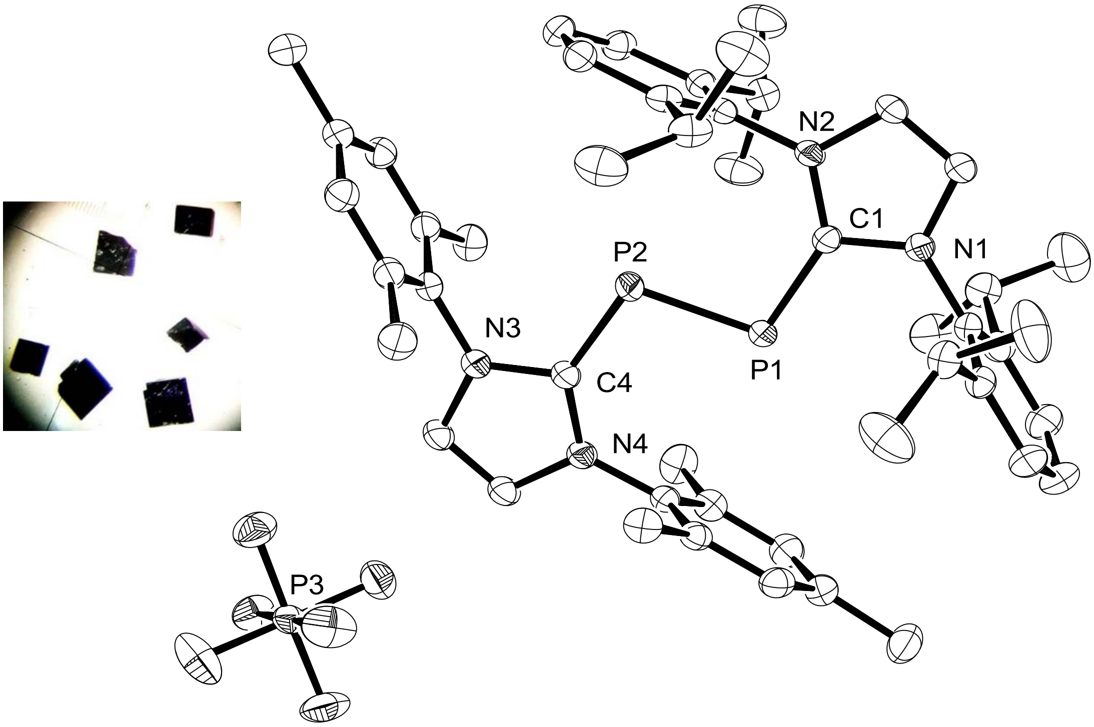

Figure S42: ORTEP diagram of the mono cationic radical **[5]**PF_6 polymorph A with thermal displacement parameters drawn at 50% probability level. Hydrogen atoms and solvent molecules are omitted for clarity. Selected bond lengths [Å]: P1–P2 2.1088(7), C1–P1 1.806(2) and C4–P2 1.797(2).

Table S3: Crystal data and structure refinement for **[5]**$PF_6\cdot 2CH_2Cl_2$ polymorph A

CCDC number	1572772	
Empirical formula	$C_{50}H_{64}Cl_4F_6N_4P_3$	
Formula weight	1069.76	
Temperature	100(2) K	
Wavelength	1.54184 Å	
Instrument (scan mode)	Oxford Diffraction Xcalibur, Atlas, Nova (ω scan)	
Crystal system	Monoclinic	
Space group	$P2_1/c$	
Unit cell dimensions	a = 18.8778(10) Å	α = 90°
	b = 16.6879(8) Å	β = 95.902(4)°
	c = 17.4336(8) Å	γ = 90°
Volume	5463.0(5) $Å^3$	
Z	4	
Density (calculated)	1.301 Mg/m^3	
Absorption coefficient	3.281 mm^{-1}	
F(000)	2236	
Crystal habitus	block (black)	
Crystal size	0.130 x 0.120 x 0.080 mm^3	
Theta range for data collection	3.543 to 76.350°	

Index ranges	-17<=h<=23, -21<=k<=20, -21<=l<=21
Reflections collected	72990
Independent reflections	11369 [R(int) = 0.0841]
Completeness to θ = 67.684°	100.0 %
Absorption correction	Gaussian
Max. and min. transmission	0.988 and 0.980
Refinement method	Full-matrix least-squares on F^2
Data / restraints / parameters	11369 / 0 / 618
Goodness-of-fit on F^2	1.024
Final R indices [I>2σ(I)]	R1 = 0.0480, wR2 = 0.1127
R indices (all data)	R1 = 0.0679, wR2 = 0.1260
Extinction coefficient	n/a
Largest diff. peak and hole	0.985 and -0.770 e.Å^{-3}
Crystallisation Details:	from dichloromethane

Measurement and Refinement Details: The crystal was slowly cooled to 100K in the nitrogen gas stream on the diffractometer starting at room temperature.

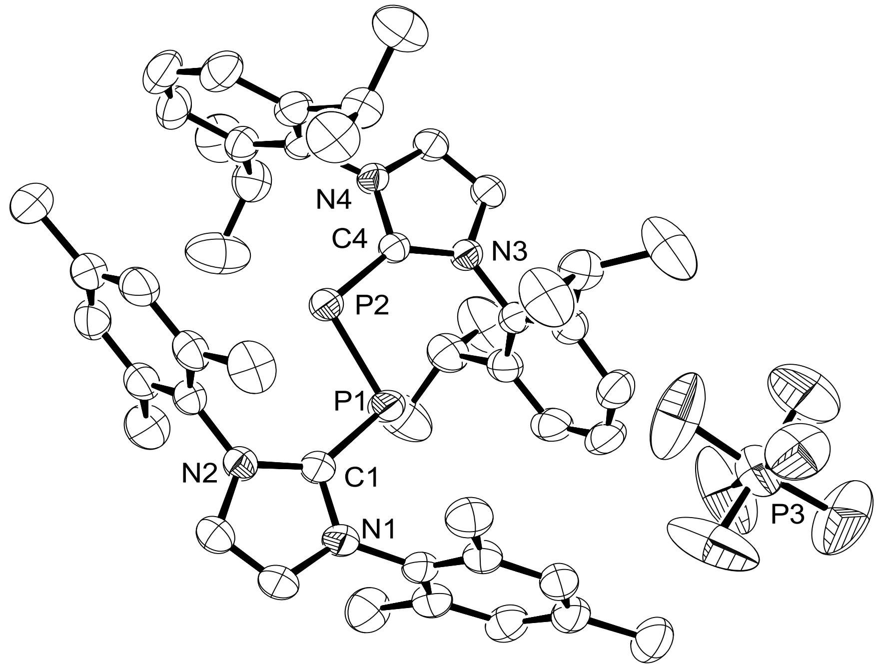

Figure S43: ORTEP diagram of the mono cationic radical **[5]**PF$_6$ polymorph B with thermal displacement parameters drawn at 50% probability level. Hydrogen atoms, solvent molecules and the minor component of the disordered PF$_6$ anion are omitted for clarity. Selected bond lengths [Å]: P1–P2 2.1065(9), C1–P1 1.791(2) and C4–P2 1.798(2).

Table S4: Crystal data and structure refinement for **[5]**$PF_6 \cdot 2CH_2Cl_2$ polymorph B

CCDC	1572771	
Empirical formula	$C_{50}H_{64}Cl_4F_6N_4P_3$	
Formula weight	1069.76	
Temperature	200(2) K	
Wavelength	1.54184 Å	
Instrument (scan mode)	Oxfrord Diffraction Xcalibur, Atlas, Nova (ω scan)	
Crystal system	Triclinic	
Space group	$P\bar{1}$	
Unit cell dimensions	a = 10.9228(4) Å	α = 67.890(4)°
	b = 14.9659(8) Å	β = 79.842(4)°
	c = 18.5836(8) Å	γ = 84.588(4)°
Volume	2769.0(2) $Å^3$	
Z	2	
Density (calculated)	1.283 Mg/m^3	
Absorption coefficient	3.237 mm^{-1}	
F(000)	1118	
Crystal habitus	irregular (black)	
Crystal size	0.230 x 0.170 x 0.150 mm^3	
Theta range for data collection	3.189 to 76.345°	
Index ranges	-13<=h<=13, -18<=k<=18, -23<=l<=22	
Reflections collected	114993	
Independent reflections	11541 [R(int) = 0.0727]	
Completeness to θ = 67.684°	100.0 %	
Absorption correction	Gaussian	
Max. and min. transmission	0.981 and 0.972	
Refinement method	Full-matrix least-squares on F^2	
Data / restraints / parameters	11541 / 36 / 682	
Goodness-of-fit on F^2	1.040	
Final R indices [I>2σ(I)]	R1 = 0.0611, wR2 = 0.1676	
R indices (all data)	R1 = 0.0850, wR2 = 0.1895	
Extinction coefficient	n/a	
Largest diff. peak and hole	0.654 and -0.893 $e.Å^{-3}$	
Crystallisation Details:	from dichloromethane and *n*-hexane	

Measurement and Refinement Details: First attempts to measure this structure at 100 K led to decomposition of the crystals, possibly because of a phase transition. Since the data quality of this structure is worse than the one of polymorph A this structure is not discussed in the manuscript.

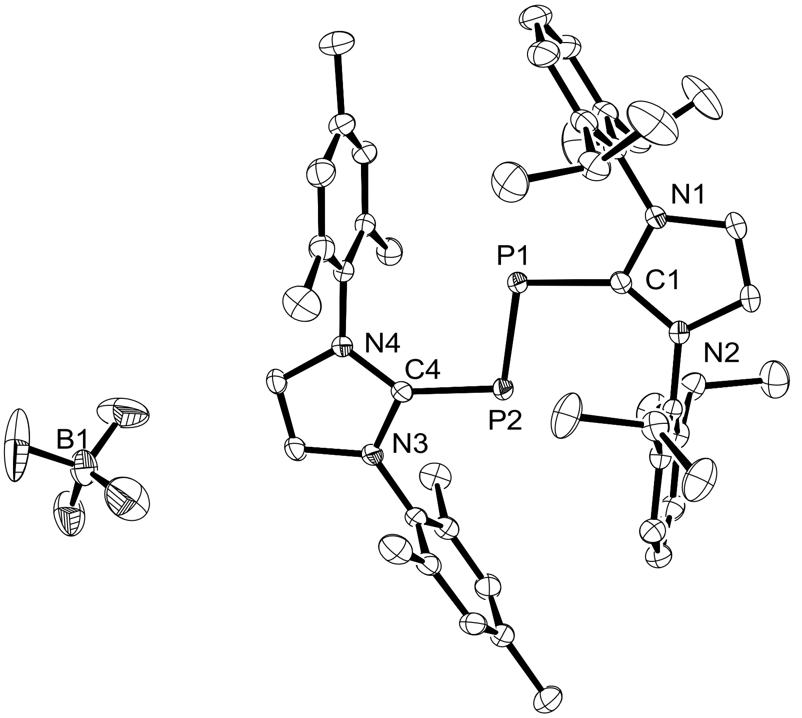

Figure S44: ORTEP diagram of the mono cationic radical **[5]**BF_4 with thermal displacement parameters drawn at 50% probability level. Hydrogen atoms, solvent molecules and the minor component of the disordered BF_4 anion are omitted for clarity. Selected bond lengths [Å]: P1–P2 2.1083(5), C1–P1 1.8054(13) and C4–P2 1.7973(13).

Table S5: Crystal data and structure refinement for **[5]**$BF_4\cdot 2CH_2Cl_2$

CCDC	1572773	
Empirical formula	$C_{50}H_{64}BCl_4F_4N_4P_2$	
Formula weight	1011.60	
Temperature	100(2) K	
Wavelength	1.54184 Å	
Instrument (scan mode)	Oxford Diffraction Xcalibur, Atlas, Nova (ω scan)	
Crystal system	Monoclinic	
Space group	*P*2$_1$/*c*	
Unit cell dimensions	a = 18.6443(2) Å	α = 90°
	b = 16.6256(2) Å	β = 96.787(2)°
	c = 17.2750(2) Å	γ = 90°
Volume	5317.25(11) Å^3	
Z	4	
Density (calculated)	1.264 Mg/m^3	
Absorption coefficient	3.008 mm^{-1}	
F(000)	2124	

Crystal habitus	cube (black)
Crystal size	0.310 x 0.290 x 0.200 mm^3
Theta range for data collection	3.573 to 76.361°
Index ranges	-23<=h<=23, -20<=k<=18, -21<=l<=21
Reflections collected	107023
Independent reflections	11089 [R(int) = 0.0514]
Completeness to θ = 67.684°	100.0 %
Absorption correction	Gaussian
Max. and min. transmission	0.966 and 0.946
Refinement method	Full-matrix least-squares on F^2
Data / restraints / parameters	11089 / 49 / 659
Goodness-of-fit on F^2	1.038
Final R indices [I>2σ(I)]	R1 = 0.0408, wR2 = 0.1091
R indices (all data)	R1 = 0.0441, wR2 = 0.1125
Extinction coefficient	n/a
Largest diff. peak and hole	0.590 and -0.689 e.Å^{-3}
Crystallisation Details:	from THF and dichloromethane layered with *n*-hexane

Measurement and Refinement Details: One BF_4 anion and one dichloromethane molecule were refined with a discrete disorder model over two positions. SADI restraints were applied. This structure is isostructural to **[5]**$PF_6 \cdot 2CH_2Cl_2$ polymorph A.

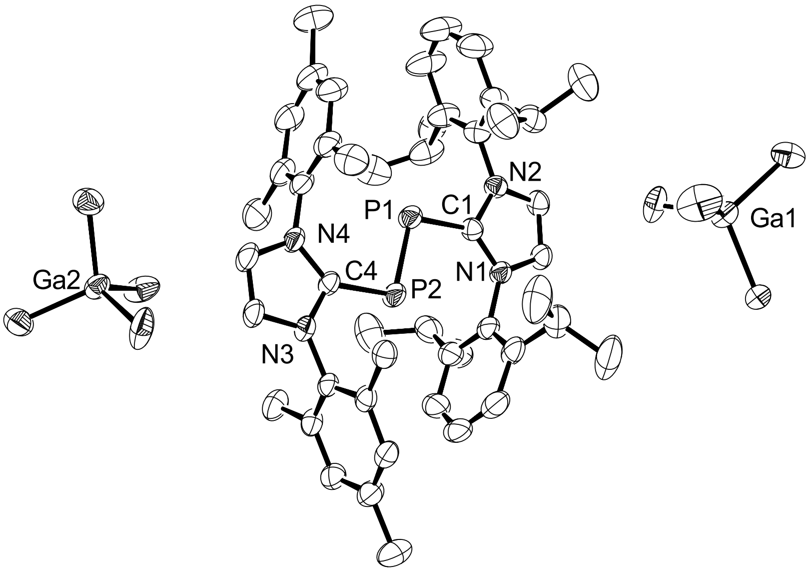

Figure S45: ORTEP diagram of **[6]**$[GaCl_4]_2$ with thermal displacement parameters drawn at 50% probability level. Hydrogen atoms and the minor component of the disordered $GaCl_4$ anions are omitted for clarity. Selected bond lengths [Å] and angles [°]: P1–P2 2.0450(11), P1–C1 1.822(3), P2–C4 1.816(3) and N1-C1-N2 106.2(2), C1-P1-P2 100.77(9) and C4-P2-P1 100.17(10).

Table S6: Crystal and structure refinement data of **[6]**$[GaCl_4]_2 \cdot 3CH_2Cl_2$ [+solvent]

CCDC	1572774	
Empirical formula	$C_{51}H_{66}Cl_{14}Ga_2N_4P_2$	
Formula weight	1432.75	
Temperature	100(2) K	
Wavelength	1.54184 Å	
Instrument (scan mode)	Oxford Diffraction Xcalibur, Atlas, Nova(ω scan)	
Crystal system	Monoclinic	
Space group	*C*2/*c*	
Unit cell dimensions	a = 21.5044(8) Å	α = 90°
	b = 13.6283(4) Å	β = 95.086(4)°
	c = 46.5389(14) Å	γ = 90°
Volume	13585.4(8) $Å^3$	
Z	8	
Density (calculated)	1.401 Mg/m^3	
Absorption coefficient	6.761 mm^{-1}	
F(000)	5840	
Crystal habitus	block (orange)	
Crystal size	0.180 x 0.090 x 0.090 mm^3	
Theta range for data collection	3.814 to 76.497°	
Index ranges	-27<=h<=27, -17<=k<=15, -57<=l<=58	
Reflections collected	147972	
Independent reflections	14127 [R(int) = 0.0694]	
Completeness to θ = 67.684°	100.0 %	
Absorption correction	Semi-empirical from equivalents	
Max. and min. transmission	1.00000 and 0.64316	
Refinement method	Full-matrix least-squares on F^2	
Data / restraints / parameters	14127 / 112 / 633	
Goodness-of-fit on F^2	1.051	
Final R indices [I>2σ(I)]	R1 = 0.0516, wR2 = 0.1167	
R indices (all data)	R1 = 0.0628, wR2 = 0.1226	
Largest diff. peak and hole	0.524 and -0.647 e.$Å^{-3}$	
Crystallisation Details:	from dichloromethane and hexane	

Measurement and Refinement Details: The structure suffers from severe disorder. The two gallium tetrachloride ($GaCl_4$) anions were refined over two positions. Three dichloromethane molecules as well as one agglomeration of residual density of unknown composition have been treated with the program SQUEEZE (part of the PLATON suite: A. L. Spek, University of Utrecht, Netherlands) to remove mathematically the residual electron density.[7] The empirical formula and derived parameters are based on three dichloromethane molecules per asymmetric unit. Since an unidentified moiety has been removed, this crystal structure is unambiguously confirming only the structural parameters of the NHC diphosphorus moiety, but not its charge.

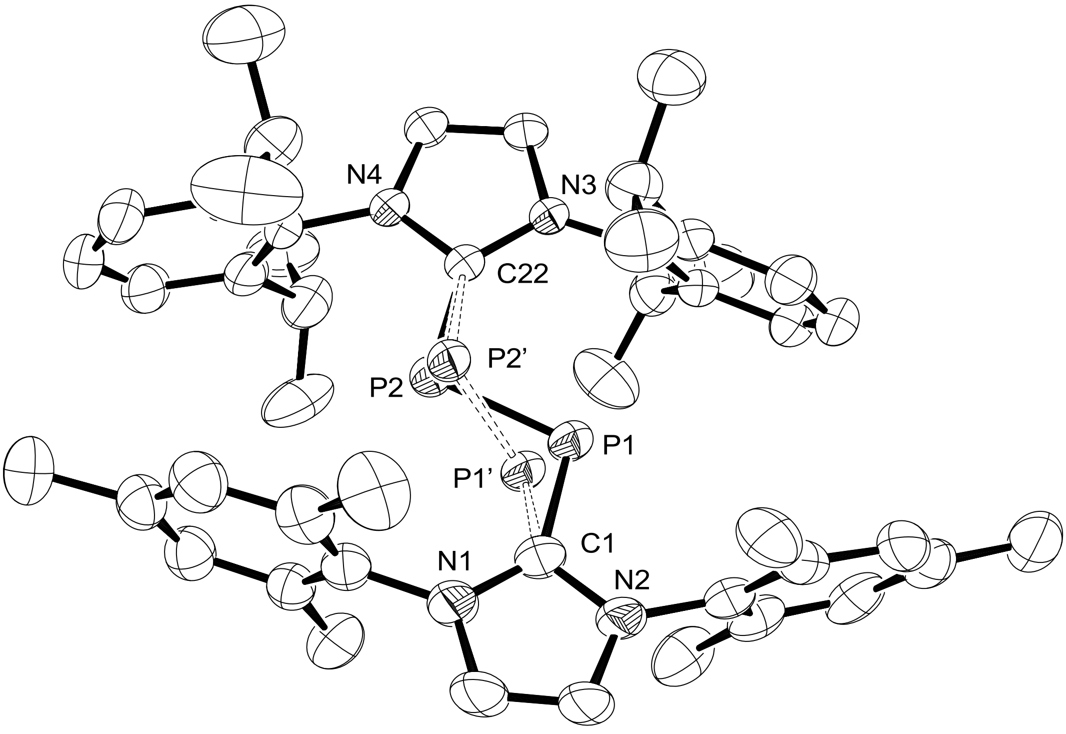

Figure S46: ORTEP diagram of the dicationic moiety of **[6]**[BAr^F]$_2$ with thermal displacement parameters drawn at 50% probability level. Hydrogen atoms, and the BAr^F anions are omitted for clarity. Selected bond lengths [Å] and angles [°]: P1–P2 2.0453(13), P1'–P2' 2.266(11), C1–P1 1.840(3), C1–P1' 1.883(7), C22–P2 1.828(3), C22–P2' 2.003(8), C1-P1-P2 100.15(12), C22-P2-P1 100.17(10), C1-P1'-P2' 89.9(4), C22-P2'-P1' 91.6(4).

Table S7: Crystal data and structure refinement for **[6]**[BAr^F]$_2$ [+solvent]

CCDC	1572775	
Sum formula	$C_{112}H_{84}B_2F_{48}N_4P_2$	
Moiety formula	$C_{48}H_{60}N_4P_2^{2+}$, 2($C_{32}H_{12}BF_{24}^{1-}$)	
Formula weight	2481.39	
Temperature	100(2) K	
Wavelength	1.54184 Å	
Instrument (scan mode)	Oxford Diffraction, Xcalibur, Atlas, Nova (ω scan)	
Crystal system, Space group	Triclinic, $P\bar{1}$ (no. 2)	
Unit cell dimensions	a = 16.1731(7) Å	α = 80.996(4)°.
	b = 19.4127(10) Å	β = 76.569(4)°.
	c = 20.26550(10) Å	γ = 69.481(4)°.
Volume, Z	5776.3(4) Å^3, 2	
Cell determination	43942 refl., 3.33° <= θ <= 75.80°	
Density (calculated)	1.427 Mg/m^3	
Absorption coefficient	1.474 mm^{-1}	
F(000)	2512	
Crystal habitus	fragment of plate (clear orange)	
Crystal size	0.21 x 0.18 x 0.04 mm^3	

Data collection	3.367° < θ < 65.996°
Completeness to θ = 65.996°	99.9 %
Index ranges	-19 <= h <= 19, -23 <= k <= 23, -24 <= l <= 24
Reflections collected / indep. / obs.	274849 / 20102 (Rint = 0.0786) / 16591
Absorption correction	Semi-empirical from equivalents
Max. and min. transmission	1.000 and 0.830
Solution method	iterative methods
Refinement method	Full-matrix least-squares on F^2
Hydrogen solution / refinement	geom / constr
Data / restraints / parameters	20102 / 228 / 1697
Goodness-of-fit on F^2	1.061
Final R indices [I>2σ(I)]	R1 = 0.0685, wR2 = 0.1888
R indices (all data)	R1 = 0.0810, wR2 = 0.1997
Largest diff. peak and hole	0.851 and -0.596 e.Å^{-3}
Weighting scheme	$w=1/[\sigma^2(Fo^2)+(0.1102P)^2+4.6446P]$ where $P=(Fo^2+2Fc^2)/3$

Measurement and Refinement Details: No appropriate model could be established for co-crystallized solvent molecules, presumably DCM; the data were processed using the SQUEEZE/PLATON program.[7] A P_2 moiety is disordered over two sites. It was refined applying a split atom model. The SOF refined to 0.866(2), a common ADP was refined for each disordered atom pair. Six disordered CF_3 groups were refined using split atom models (0.64(1), 0.596(9), 0.70(1), 0.81(2), 0.73(2), 0.887(8) SOF of main components). Similarity restraints were applied (SAME); the ADPs were restrained to approximate isotropic behavior (ISOR).

D) Computational details

All computations were performed using the density functional method B97-D (*S. Grimme*) as implemented in the Gaussian09 program.[8] For all main group elements (C, H, Cl and P) the all-electron triple-ζ basis set (6-311G**) was used.[9] Natural Bond Orbital (NBO) analysis (NBO charges, WBI) was carried out using NBO version 3,[10] which is part of the **Gaussian09** program package and all ***relaxed force constants*** (**RFC** in N/cm) were calculated as the reciprocal of the corresponding **compliance constants** (**CC** in Å/mdyn) using the program ***Compliance 3.0***.[11] For quantitative analysis of the spin density and for calculation of the Mayer bond order the free software ***Muliwfn*** was used.[12]

Table S8: Energies for all optimized structures

Compound	$E_{0K}{}^{a}$ [Ha]	$E_{298K}{}^{b}$ [Ha]	$H_{298K}{}^{b}$ [Ha]	$G_{298K}{}^{b}$ [Ha]
3 [(IPr)PPCl(IMes)]$^+$	-3225.180025	-3225.119772	-3225.118828	-3225.275294
3' [(IMes)PPCl(IPr)]$^+$	-3225.180623	-3225.119897	-3225.118952	-3225.279413
4	-2765.068422	-2765.009292	-2765.008348	-2765.164137
5$^{+\cdot}$	-2764.914495	-2764.855705	-2764.854761	-2765.010597
6^{2+}	-2764.629372	-2764.570598	-2764.569654	-2764.725161

[a] DFT energy incl. ZPE.

[b] standard conditions T = 298.15 K and p = 1 atm.

Table S9a: NBO Analysis of selected Atoms and Bonds of complex **4**

	NBO no.	type	element	NBO charge	WBI	Mayer BO	compl. const.	relax force const.	coefficent	localization [%]	AO contribution [%]		
											s	p	d
$[(IMes)P_2(IPr)]$ **(4)**	202	$\pi(P\text{-}C_{IMes})$	P						0.79	63	0	100	0
			C						0.61	37	0	100	0
	201	$\pi(P\text{-}C_{IPr})$	P						0.79	62	0	100	0
			C						0.62	38	0	100	0
	183	$\sigma(P\text{-}P)$	P_{IPr}		1.03	0.79	0.662	1.511	0.71	50	13	87	0
			P_{IMes}						0.71	50	13	87	0
	182	$LP(P_{IMes})$	P	-0.03	---				1	100	71	29	0
	181	$LP(P_{IPr})$	P	-0.01	---				1	100	71	29	0
	112	$\sigma(P\text{-}C_{IPr})$	P		1.35	1.38	0.302	3.311	0.57	33	18	82	1
			C	0.07					0.82	67	44	56	0
	111	$\sigma(P\text{-}C_{IMes})$	P		1.33	1.35	0.303	3.300	0.57	33	18	82	1
			C	0.06					0.82	67	44	56	0

Table S9b: Surface plots of selected NBOs of complex **4**

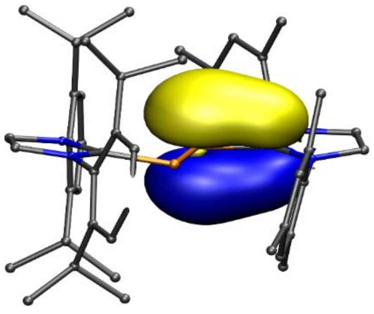

NBO #202 [π(C–P)]

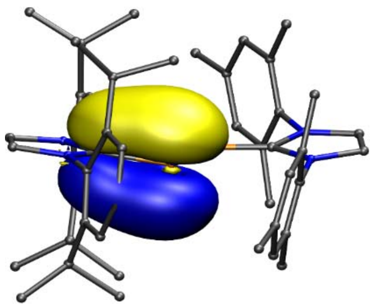

NBO #201 [π(C–P)]

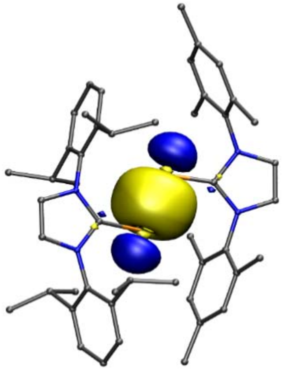

NBO #183 [σ(P–P)]

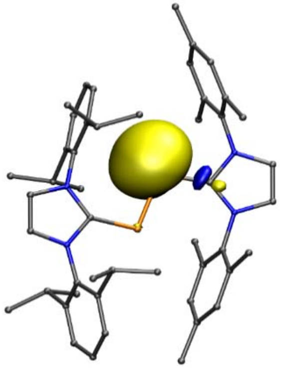

NBO #182 [LP(P)]

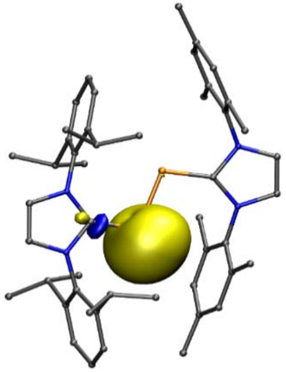

NBO #181 [LP(P)]

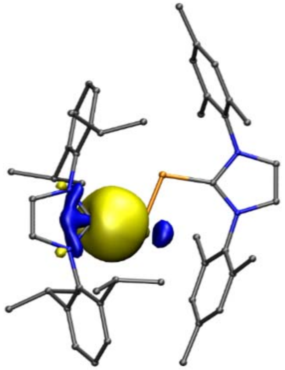

NBO #112 [σ(C–P)]

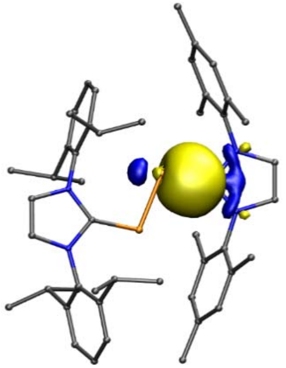

NBO #111 [σ(C–P)]

Table S10a: NBO Analysis of selected Atoms and Bonds of complex **5**$^{+\cdot}$

	NBO no.	type	element	NBO charge	WBI	Mayer BO	compl. const.	relax force const.	coefficent	localization [%]	AO contribution [%]		
											s	p	d
[(IMes)P$_2$(IPr)]$^{+\cdot}$ (**5**$^{+\cdot}$)	203	P$_{IMes}$	P		---				1	100	1	99	0
	202	P$_{IPr}$	P	0.13	---				1	100	0	100	0
	148	P$_{IMes}$	P	0.12	---				1	100	73	27	0
	140	σ(P-P)	P$_{IPr}$		1.23	0.95	0.496	2.016	0.70	50	13	87	0
			P$_{IMes}$						0.71	50	14	86	0
	134	P$_{IPr}$	P		---				1	100	71	29	0
	108	σ(P-C$_{IPr}$)	P		1.08	1.08	0.382	2.618	0.57	33	14	85	1
			C	0.12					0.82	67	42	58	0
	106	σ(P-C$_{IMes}$)	P		1.12	1.15	0.361	2.770	0.58	33	15	84	1
			C	0.12					0.82	67	41	59	0

Table S10b: Surface plots of selected NBOs of complex $\mathbf{5}^{+\cdot}$

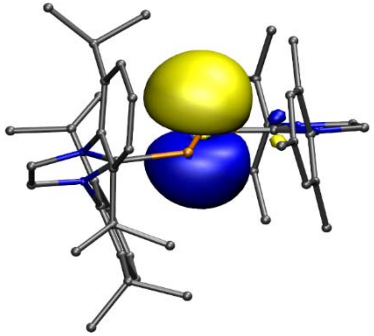
NBO #203 [SOMO, P_{IMes}]

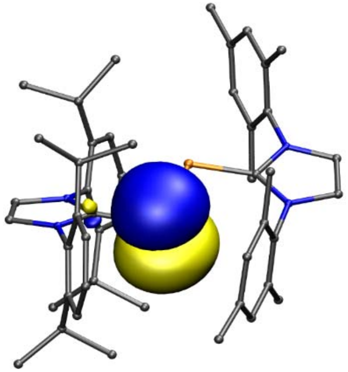
NBO #202 [P_{IPr}]

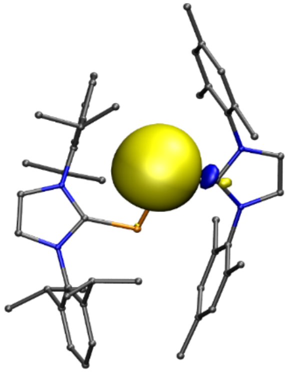
NBO #148 [P_{IMes}]

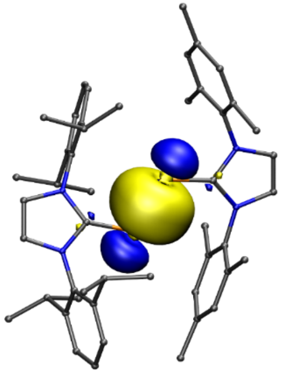
NBO #140 [σ(P–P)]

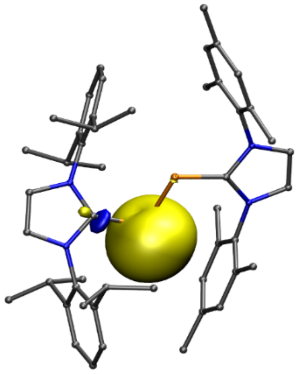
NBO #134 [P_{IPr}]

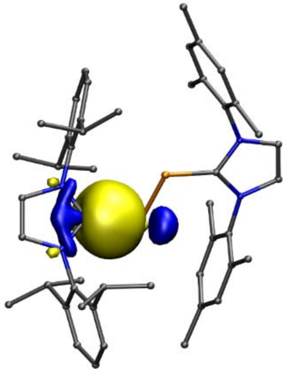
NBO #108 [σ(C–P)]

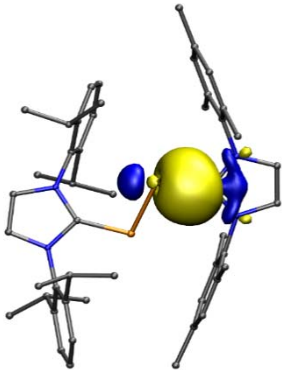
NBO #106 [σ(C–P)]

Table S11a: NBO Analysis of selected Atoms and Bonds of complex **6**$^{2+}$

	NBO no.	type	element	NBO charge	WBI	Mayer BO	compl. const.	relax force const.	coefficent	localization [%]	AO contribution [%]		
											s	p	d
$[(\mathrm{IMes})\mathrm{P_2}(\mathrm{IPr})]^{2+}$ (**6**$^{2+}$)	203	π*(P-P)	P_{IPr}										
			P_{IMes}										
	190	π(P-P)	P_{IPr}						0.71	50	0	100	0
			P_{IMes}						0.70	50	0	100	0
	127	LP(P_{IPr})	P	0.33	---				1	100	74	26	0
	126	LP(P_{IMes})	P	0.37	---				1	100	71	29	0
	125	σ(P-P)	P_{IPr}		1.67	1.37	0.377	2.653	0.70	49	14	86	1
			P_{IMes}						0.71	51	16	84	1
	104	σ(P-C_{IPr})	P		0.95	0.93	0.404	2.475	0.57	33	13	86	1
			C	0.13					0.82	67	39	61	0
	101	σ(P-C_{IMes})	P		1.01	1.03	0.392	2.551	0.58	33	14	85	1
			C	0.12					0.82	67	39	61	0

Table S11b: Surface plots of selected NBOs of complex **6**$^{2+}$

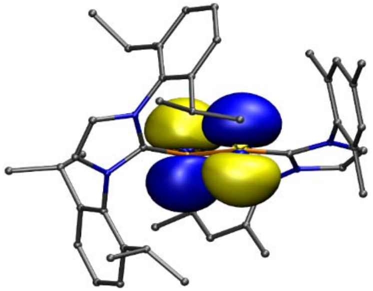

NBO #203 [π*(P–P)]

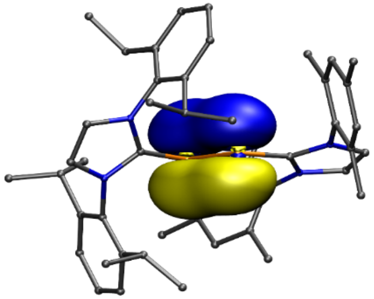

NBO #190 [π(P–P)]

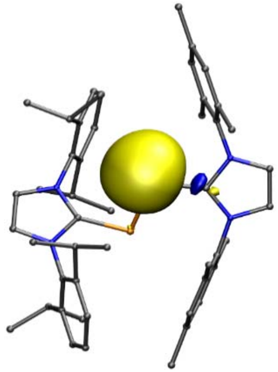

NBO #127 [LP(P)]

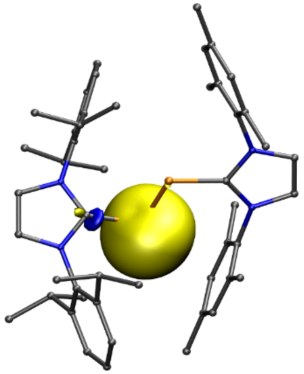

NBO #126 [LP(P)]

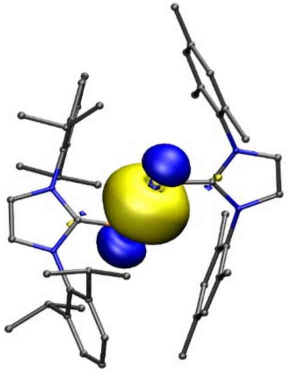

NBO #125 [σ(P–P)]

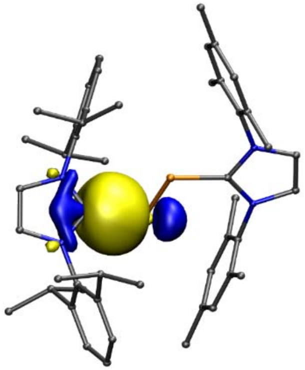

NBO #104 [σ(C–P)]

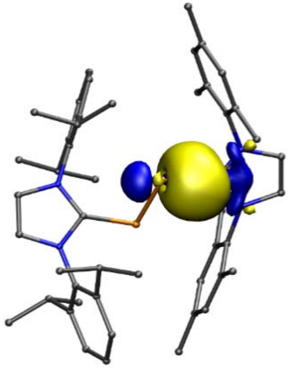

NBO #101 [σ(C–P)]

E) References

[1] Y. Wang, Y. Xie, M. Y. Abraham, R. J. Gilliard, P. Wei, H. F. Schaefer III and P. v. R. Schleyer, G. H. Robinson, *Organometallics*, 2010, **29**, 4778.

[2] A. Doddi, D. Bockfeld, T. Bannenberg, P. G. Jones and M. Tamm, *Angew. Chem. Int. Ed.*, 2014, **53**, 13568.

[3] S. Stoll and A. Schweiger, *J. Magn. Reson.*, 2006, **178**, 42.

[4] *CrysAlisPRO*; Oxford Diffraction /Agilent Technologies UK Ltd, Yarnton, England.

[5] a) G. M. Sheldrick, *Acta Crystallogr, Sect. A*, 2008, **64**, 112; b) G. M. Sheldrick, *Acta Crystallogr, Sect. A*, 2015, **71**, 3.

[6] Y. Wang, Y. Xie, P. Wei, R. B. King, H. F. Schaefer III, P. v. R. Schleyer and G. H. Robinson, *J. Am. Chem. Soc.*, 2008, **130**, 14970.

[7] A. L. Spek, *Acta Crystallogr., Sect. C: Struct. Chem.* 2015, **71**, 9-18.

[8] Gaussian 09, Revision A.1, M. J. Frisch, G. W. Trucks, H. B. Schlegel, G. E. Scuseria, M. A. Robb, J. R. Cheeseman, G. Scalmani, V. Barone, B. Mennucci, G. A. Petersson, H. Nakatsuji, M. Caricato, X. Li, H. P. Hratchian, A. F. Izmaylov, J. Bloino, G. Zheng, J. L. Sonnenberg, M. Hada, M. Ehara, K. Toyota, R. Fukuda, J. Hasegawa, M. Ishida, T. Nakajima, Y. Honda, O. Kitao, H. Nakai, T. Vreven, J. A. Montgomery, Jr., J. E. Peralta, F. Ogliaro, M. Bearpark, J. J. Heyd, E. Brothers, K. N. Kudin, V. N. Staroverov, R. Kobayashi, J. Normand, K. Raghavachari, A. Rendell, J. C. Burant, S. S. Iyengar, J. Tomasi, M. Cossi, N. Rega, J. M. Millam, M. Klene, J. E. Knox, J. B. Cross, V. Bakken, C. Adamo, J. Jaramillo, R. Gomperts, R. E. Stratmann, O. Yazyev, A. J. Austin, R. Cammi, C. Pomelli, J. W. Ochterski, R. L. Martin, K. Morokuma, V. G. Zakrzewski, G. A. Voth, P. Salvador, J. J. Dannenberg, S. Dapprich, A. D. Daniels, Ö. Farkas, J. B. Foresman, J. V. Ortiz, J. Cioslowski, and D. J. Fox, Gaussian, Inc., Wallingford CT, **2009**.

[9] X. Cao and M. Dolg, *J. Chem. Phys.*, 2001, **115**, 7348.

[10] a) J. P. Foster and F. Weinhold, *J. Am. Chem. Soc.*, 1980, **102**, 7211; b) A. E. Reed and F. Weinhold, *J. Chem. Phys.*, 1983, **78**, 4066; c) A. E. Reed, R. B. Weinstock and F. Weinhold, *J. Chem. Phys.*, 1985, **83**, 735; d) A. E. Reed and F. Weinhold, *J. Chem. Phys.*, 1985, **83**, 1736.

[11] a) K. Brandhorst and J. Grunenberg, *J. Chem. Phys.*, 2010, **132**, 184101; b) K. Brandhorst and J. Grunenberg, *Chem. Soc. Rev.*, 2008, **37**, 1558.

[12] T. Lu, Multiwfn (Version 3.4) - A Multifunctional Wavefunction Analyzer, https://multiwfn.codeplex.com/.